SWS Miscellaneous Publication 150

Flood Reconstruction in Southern Illinois Using Tree Rings

by
Susan A. Loomans

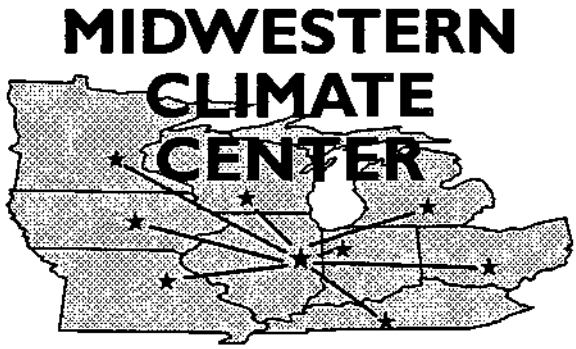

Midwestern Climate Center
Climate Analyais Center
National Weather Service
National Oceanic and Atmospheric Administration

Illinois State Water Survey
A Division of the Dept. of Energy and Natural Resources

MCC Research Report 93-02
August 1993

FLOOD RECONSTRUCTION IN SOUTHERN ILLINOIS USING TREE RINGS

BY

SUSAN MARIE LOOMANS

B.S, United States Air Force Academy, 1987
B.S, Texas A & M University, 1988

THESIS

Submitted in partial fulfillment of the requirements
for the degree of Master of Science in Geography
in the Graduate College of the
University of Illinois at Urbana-Champaign, 1993

Urbana, Illinois

TABLE OF CONTENTS

LIST OF FIGURES

LIST OF TABLES

Table

CHAPTER 1
INTRODUCTION

Water management is a crucial element in directing future land development across the United States. Measures are often taken to minimize flood hazards while at the same time maintaining an adequate water supply for consumption, irrigation, sewage treatment and aquifer regeneration (Stockton, 1975). Water resource management activities directed at regulating stream runoff must address a wide variety of considerations, including the frequency and magnitude of floods. The confidence of flood frequency analysis is dependent on the existence and length of gaged records (Kochel and Baker, 1982; Martens, 1992). A lack of long-duration hydrologic records for United States streams has limited the confidence of flood frequency estimates, and created an opportunity for data contributions by proxy methods.

The science of tree-ring analysis, or dendrochronology, can provide a valuable source of paleoflood information (Martens, 1992; McCord, 1990; Sigafoos, 1964). The year and, often, magnitude of significant floods can be determined from the annual ring by considering the geomorphic situation and biological response of trees to flooding. The growth of tree rings primarily depends on soil nutrients (nitrogen, phosphorous, potassium, calcium, magnesium, and sulfur), and climatic factors (mainly temperature and soil moisture)(Kramer and Kozlowski, 1960). By calibrating ring growth to recorded weather and discharge data, tree-ring information can be used to reconstruct yearly variations in climate. These relationships can be applied through the life of the tree, thus extending recent climatic and hydrologic records back in time (Fritts, 1976).

1.A. Purpose and scope

The purpose of this study is to demonstrate how tree-ring analysis along rivers can provide valuable pre-historic flood frequency and magnitude information. The Big Muddy River of southern Illinois was selected as a candidate for paleoflood research. Justification for its selection, and specific objectives and hypotheses follow.

1.A.1 Justification for research

The Big Muddy River, a tributary of the Mississippi River, lies in a region which is historically prone to flooding. Major floods since the turn of the century have resulted in significant loss of property and life, and prompted numerous flood control projects. The scope of these projects were based on flood information from gaged records, which did not generally begin in the area in earnest until after 1910. To base flood magnitude and frequency estimates on such a limited observed record is insufficient, since the variance of the gaged period may not be representative of the variance over longer time periods. Long period variance is often the best

predictor for future events, since it has increased potential to encompass extremes and minor fluctuations which may someday be repeated.

To date, there has been little effort to reconstruct long period variance of discharge on the Big Muddy River, or in the Upper Mississippi River valley. Such research has potential economic value, since increasing land development is forcing drainage districts to assess their ability to handle high flow events, while maintaining adequate water levels when precipitation is low. Large tracts of residential, commercial, and agricultural land lie on floodplains and are vulnerable to floods, so it is important to improve our understanding of flood potential. But since resources are limited, the costs and benefits of flood control projects must be carefully weighed. The most important elements in project design are flood magnitude and frequency, which together can be used to calculate risks that future flood events will exceed protection limits. An extension of the hydrologic record using tree rings can provide more complete information on flood risks, and therefore better direction for measured flood control.

1.A.2 Objective

The objective of this research is to reconstruct past river discharge and flood events on the Big Muddy River using dendrochronology. Suitable trees were located in the Shawnee National Forest, and climatic and hydrologic data for the past 60 years were available for initial calibration.

The following questions are addressed: How does tree growth at various levels on and above the floodplain reflect flood events? What do these relationships infer about past river behavior? And finally, what applications are there to other developing areas in Illinois or the Upper Mississippi River valley?

1.A.3 Hypotheses

The general working hypothesis for this research is that flow history can be reconstructed from the tree-ring record by developing a model which correlates recent tree-ring growth with recent hydrologic data. The sampling and measurement of tree cores, statistical manipulation of ring widths, and model development will be explained later.

Hypotheses specific to the study are that tree-ring analysis on floodplains and terraces enables:

a *Determination of a prehistoric flood chronology:* Years in which flooding occurred are identified for the period of the tree-ring chronology.

b. *Estimation of flood heights:* Heights of flood scars on trees above the floodplain, elevation of flood-ringed trees above the floodplain, and comparison of tree-ring

indices from different levels on and above a floodplain serve as rough estimates of flood heights for the field site river, assuming that significant floodplain degradation or aggradation did not occur during previous decades.

c. *Reconstruction of mean monthly discharge:* Correlation and regression of tree-ring growth on gaged discharge data provides a mathematical means of estimating mean monthly discharge from ring width.

1.A.4 Organization of the thesis

Chapter 1 presents the study hypotheses, and provides background information on how paleoflood information is stored in tree rings. Current methods and applications of dendrochronology are discussed.

Chapter 2 introduces the study site where flood research was conducted. A geomorphic analysis and recent flood history of the area is included.

Chapter 3 describes methods of data acquisition and analysis. Tree core collection is presented along with sources and quality of hydrologic and climatic data. Model development and related statistics are outlined. r.

Chapters 4 and 5 discuss the results and conclusions of the flood reconstruction project, as well as the impact of such information on future planning.

Before proceeding with any scientific research, it is important to have an understanding of the basic concepts and methods in the area of study. Therefore, the remainder of this introductory chapter is devoted to outlining important points in dendrochronology, modern flood analysis, and paleoflood analysis.

1.B Concepts in dendrochronology

A review of prevalent themes in dendrochronology outlines the current framework for climatic reconstruction. Concepts in dendrochronology related to paleohydrology are discussed to provide direction for future dendrohydrologic research on Illinois river systems.

1.B.1 Tree response to climatic inputs

Tree-ring growth represents a year-long integration of its environment (Fritts, 1965). Although total seasonal growth is the result of many interacting factors, only one environmental factor dominates in limiting growth, i.e., available soil moisture during the growing season (Stokes and Smiley, 1968; LaMarche, 1974; Phipps, 1972; Stockton, 1975). Wider rings

generally correspond to a moist, cool year; while narrow rings depict dry and/or warm conditions (Fritts, 1965).

Ring widths are determined by a yearly flush of growth that begins in spring and ends in summer (Figure 1). During the early part of the growing season, large "early wood" cells are produced. Toward the middle and end of the season, growth slows, and smaller, thin-walled "latewood" cells are formed. The boundary between annual rings is marked by the abrupt shift from latewood to earlywood cells. The width and character of the annual rings is dependent not only on climatic inputs, but site and species characteristics as well.

1.B.2 The importance of site selection

Site selection in paleoflood research aims to sample trees whose growth is sensitive to changes in hydrologic parameters. Trees on well drained sites (such as slopes or terraces) are more sensitive to changes in precipitation since they are shallow-rooted and readily affected by a rapid change in soil moisture supply (Stockton, 1975; Smith and Stockton, 1981). These trees tend to exhibit a varying, or "sensitive" ring-width series (Figure 2). Poorly drained sites (such as floodplains) usually realize optimum conditions for growth, and a "complacent" ring-width series, which varies little from year to year. Complacency in floodplain trees can be interrupted if flooding saturates the soil and limits the delivery of oxygen to the roots (Fritts, 1965b). Lack of oxygen in the soil leads to accumulation of carbon-dioxide and toxic metabolic products that can inhibit growth of the tree or cause injury to living cells (Gill, 1970). The degree of flood-related impact on a tree's growth is highly dependent upon tree species and timing and duration of flooding (Gill, 1970; Hosner and Boyce, 1962).

1.B.3 The importance of species selection

Tree species selection is important since various species do not respond to flooding in the same way. Also, bottomland trees have different tolerances to saturated soils (Hosner and Boyce, 1962; Phipps, 1972). Some species thrive in saturated conditions while others suffer limited growth or even death. In addition, tree selection for coring and study must be grouped by species to eliminate species-related growth variations (Fritts, 1976).

For most deciduous species, flooding affects ring growth only when it occurs during the growing season (Gill, 1970; McAlpine, 1961). This is mainly because oxygen demand by the roots is minimal in winter (Gill; 1970). Dormant season flooding, however, may lead to increased soil moisture for the start of the following growing season. Duration of flooding during the growing season is very important, as tolerances vary dramatically with species and tree age. Seedlings and young trees are most sensitive to inundation, since their root systems are less developed (Gill, 1970; Hosner and Boyce, 1962).

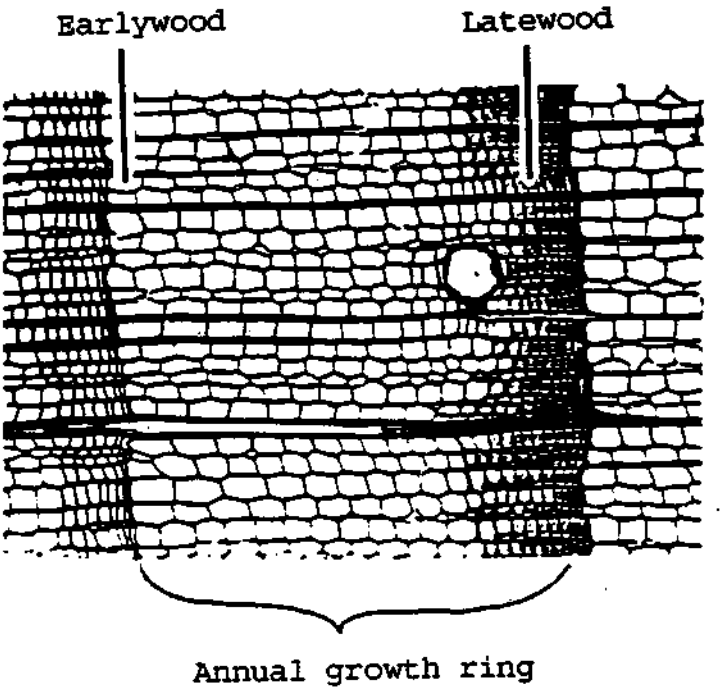

Figure l. Annual ring growth (from Stokes and Smiley, 1968).

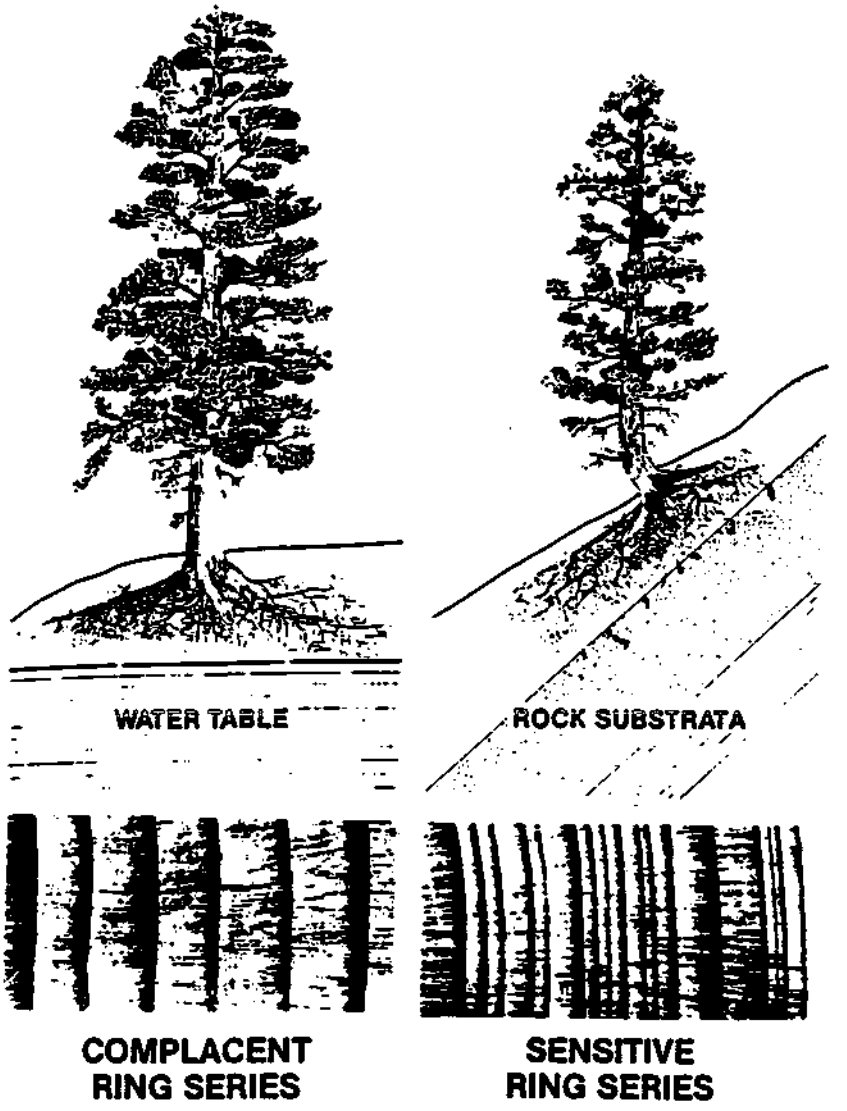

Figure 2. Site influence on tree sensitivity (from Stokes and Smiley, 1968).

In addition to understanding the biological response of trees to flooding, it is important to comprehend magnitude and frequency estimation.

1.C Magnitude and frequency of floods

A key component to floodplain management is flood frequency estimation, which is the probability of occurrence for a flood to exceed a given magnitude (Knighton, 1984). Recurrence interval, the reciprocal of frequency, is the mean number of years separating flood events.

The conventional method of flood frequency estimation uses an annual maximum flood series, in which the highest peak discharge of each water year is listed in an array that is ranked to size from largest to smallest. The return period for a particular year's peak discharge is computed as

$$T=(n+l)/m$$

where T is return period (years), n is number of years of record, and m is rank within the series (Knighton, 1984).

The return period estimate is limited by the length of the flood series record, with a maximum return period of n+1 years for the largest (m=l) flood in the series. Return periods greater than n+1 years can be estimated by graphically extending a logarithmic flood frequency curve to the desired probability (Kite, 1977). Uncertainty is added by assuming that the form of the extending curve remains the same for rare events. In addition, these return period estimates could be inaccurate because the period of gaged discharge may not be representative of longer period discharge. The gaged period may be shorter than return periods of particularly destructive floods, or coincide with anomalous climatic conditions (Kochel and Baker, 1982; Hirschboeck, 1987). To illustrate, a calculated 50 year flood event from a 49 year-long gaged record could in fact be a 100 or 200 year event that just happened to occur in the gaged period. There is no guarantee that the expected number of "return" years will separate flood events. Ideally, a time series should be long enough to encompass the full range of discharge fluctuations. Realistically, gaged records must be extended with proxy data to make return period estimates with greater confidence.

A proven source of proxy flood data is dendrochronology. Current techniques will be discussed in the remainder of this chapter.

1.D Paleoflood analysis using tree rings

Dendrochronology can potentially provide two types of hydrologic information: 1) years of extreme hydrologic events such as floods or droughts, and 2) a paleoclimatic record useful for extending hydrologic records and estimating trends and variability of precipitation and discharge

(Stockton, 1975). A number of analysis techniques exist and have been proven effective. The most common approaches are described below:

1.D.1 Flood rings

Years of prolonged flooding in riparian areas can be determined with the discovery of "flood rings". Flood rings are identified by abnormalities in the wood tissue of the flooded season's growth ring (Gill, 1970; Yanosky, 1983; Martens, 1992). The abnormalities appear as enlarged cells, similar to early wood cells, but formed in a non-early wood portion of the growth ring (Figure 3). The enlarged cells form when 1) trees produce a second crop of leaves during the growing season, or when 2) rapid shoot elongation occurs and new leaves are formed at stem tips (Yanosky, 1983; Phipps, personal communication, 1993).

The first flood ring type occurs with some degree of crown inundation, where trees are partially or totally defoliated. If injury occurs early enough in the growing season, growth will continue with formation of new leaves. Hormonal release from refoliation often causes development of large vessels in the growth ring (Yanosky, 1983).

The second type of flood ring is also related to flooding, though non-injurious to a tree. Root inundation for a few days may result in rapid growth fueled from added moisture (Phipps, personal communication, 1993). Hormones released from new leaf growth at stem tips may cause a band of large cells (called "white" rings) to be formed in the growth ring, often as an extension of the earlywood zone (Yanosky, 1983).

Flood rings can be discovered, should they exist, through extensive tree coring of floodplain forests. Cores from about 10 or more flood-prone trees must be carefully examined under a microscope for growth abnormalities. Annotation of abnormal growth years shows flood frequency, highlighting common years of flood evidence from floodplain trees. The time of year when flooding occurred can be determined by noting the intra-ring position of the flood ring relative to the total ring width, which gives the approximate time of flooding during the growing season (Yanosky, 1983). Comparison of tree base heights on uneven floodplains may give information on flood magnitude, once elevations of affected trees are identified for flood years.

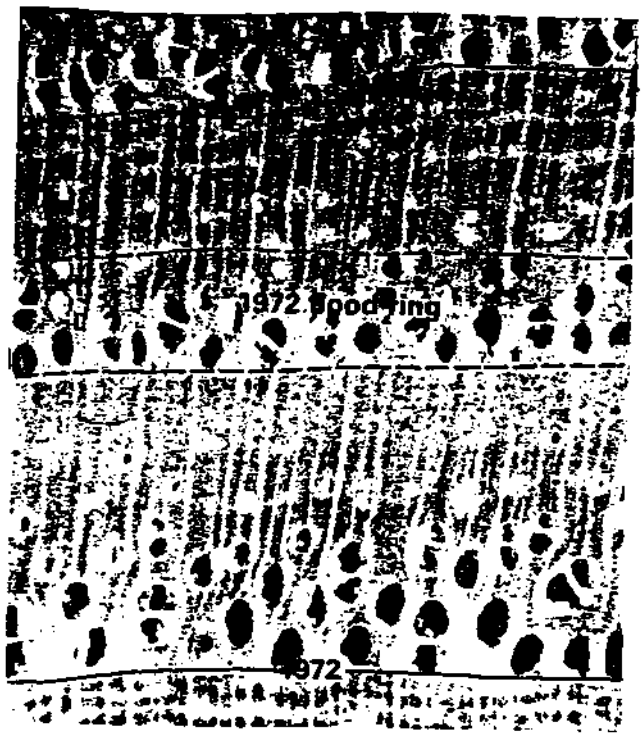

Figure 3. Flood ring composed of enlarged vessels in the latewood, having the appearance of a false ring (from Yanosky, 1983).

1.D.2 Flood scars

Years of flooding can also be determined through flood scar analysis. High discharge events have the ability to transport large quantities of debris at high velocities. When over-bank flooding occurs, floodplain trees are vulnerable to physical damage on the upstream side by floating logs or other materials rolling on the bed. Damage is most likely to occur at peak discharge, when logs are being entrained into the flow. Trees adjacent to the channel are at highest risk since logs are first intercepted there, and velocity slows further inland (Gottesfeld and Johnson-Gottesfeld, 1990). The most common types of tree damage are uprooting, breaking, shearing, and scarring (Sigafoos, 1964).

A scarring blow to the tree stem results in injury to the bark and vascular cambium (Figure 4). The bark and dead tissue are naturally sloughed off and replaced by callus tissue, which begins to cover the exposed wood from the margins (McCord, 1990; Sigafoos, 1964). Eventually the scarred area is healed over, and complete annual rings once again encircle the stem.

Tree scars can be dated by either of two methods. The first approach is to core the damaged tree and count the number of rings in from the bark to the last sound ring before scarring. Dating is also possible after coring through the scar, marking the damaged ring, and cross-dating that ring with undamaged sections of the tree.

Flood scar analysis was applied by Sigafoos (1964) to date flood events on the Potomac River in Virginia, where evidence from 28 floods were found in stems of ash trees. Techniques can also be applied to remote, pooriy-gaged rivers. Major flood events and channel changes over the past 105 years were documented for the Morice River, a braided gravel-bed river in British Columbia, using flood scars and forest stand establishment dates (Gottesfeld and Johnson-Gottesfeld, 1990).

Measurements of scar-heights are a source of paleostage data, which enables a crude estimate of past discharge. Surveyed channel dimensions and scar-heights in Rattlesnake Canyon, Arizona, have been used to compute paleodischarge for a number of flow depths (McCord, 1990).

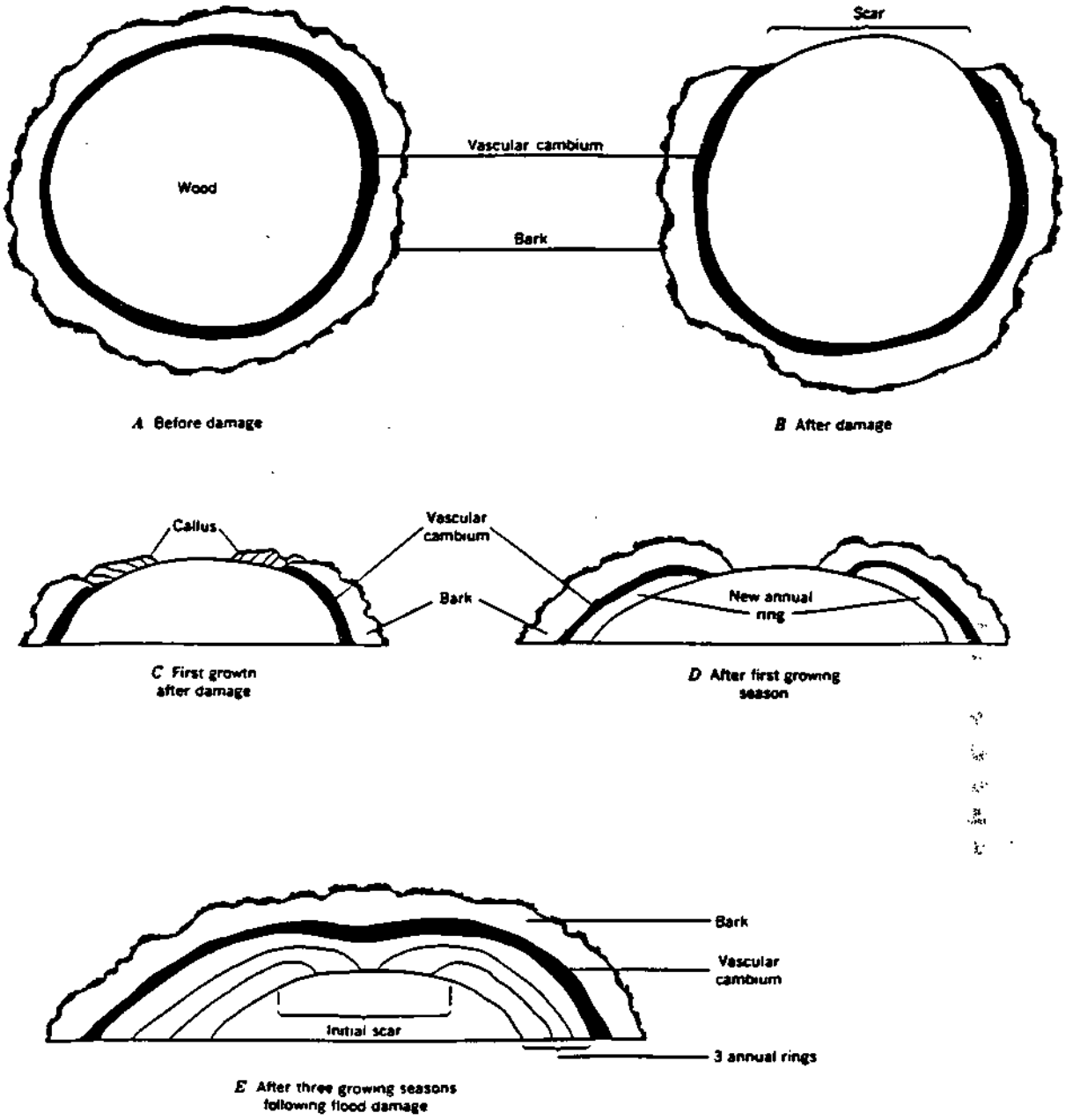

Figure 4. Illustrations of (a) undamaged tree (b) tree injured by physical impact from flooding, (c,d) formation of callus tissue, (e) healed flood scar (after Sigafoos, 1964).

1.D.3 Floodplain-upland comparisons

The effects of discharge on tree-ring growth can be isolated by analyzing ratios of annual floodplain tree-ring growth over annual upland growth (Wendland and Watson-Stegner, 1983). This technique is based on the premise that while trees from both sites experience the same climate, trees located on flooded soil potentially have comparatively wider or narrower rings than upland trees. The added soil moisture from flooding may lead to a flush of growth and an abnormally wide ring. With extended duration floods, prolonged soil saturation during or just prior to the growing season may cause a lack of oxygen transfer to the roots and inhibited ring growth for that year (Mitsch and Rust, 1984; Gill, 1970; Hosner and Boyce, 1962). A floodplain/upland ratio near 1.0 indicates no flooding for that growing season. A ratio which is significantly less or greater than 1.0 shows that one or more growth-altering floods were present on the floodplain during the spring or summer of that year.

This type of study requires core sampling from the floodplain and a number of topographic elevations above it. Tallying years with ratios less than one enables flood frequency calculations, while the upland extent of flood-inhibited rings may yield magnitude information.

1.D.4 Time series analysis

The year-to-year sequence of ring widths can be expressed as a time series for statistical analysis. Standardization techniques enable combination of individual time series into an averaged chronology representative of a number of trees. Then, statistical techniques such as correlation, principal components, and regression can be applied to determine possible causal relationships between tree-ring growth and environmental variables (Fritts, 1976).

The tree-ring time series can be used to reconstruct the discharge time series, and patterns or trends can be identified. For example, time series analysis has shown that California has experienced fewer extreme droughts during the twentieth century than in previous centuries (Hughes and Brown, 1992). Tree-ring chronologies developed from cores of big-cone spruce, used to reconstruct precipitation variability, show major fluctuations of variability over the past few thousand years. The chronologies showed the modern period of 1920-1965 to be relatively dry with low variability, with signs that conditions may be becoming more variable again (Michaelsen, et al., 1987).

Despite the fact that dendrochronology has impressive dating accuracy compared to other methods of paleo-study, there are certain limitations that must be considered when interpreting results.

1.D.5 Limitations of flood reconstruction

Under maximum stress conditions, tree growth for a particular year largely depends on that year's moisture input. More commonly, a combination of soil moisture and biological "carry-overs" result in a lag effect (auto- correlation), with a particular year's growth being influenced by moisture from the previous one or two years (Smith and Stockton, 1981). Time series analyses show that a one to two year lag correlates best with hydrologic discharge records (Wendland and Watson-Stegner, 1983). Autocorrelation can create uncertainty in the flood information stored in tree rings. Although one can account for a growth lag in the current data, it cannot be assumed that this lag will apply in the same manner throughout the reconstructed hydrology.

CHAPTER 2
STUDY AREA

2.A Basin description

The trees studied are located on floodplain and bluffs east of the Big Muddy River where it flows through the Shawnee National Forest (Figure 5). Draining an area of 5618 km^2, the Big Muddy originates in Jefferson County, Illinois, and flows southwestward for 248 km to join the Mississippi River near Grand Tower (Illinois Environmental Protection Agency, 1988). The study site for this research is located about 12 km upstream of the Big Muddy-Mississippi confluence. The lower 30 km of the Big Muddy, which includes the study site, hugs the east wall of a wide valley until it sharply turns west toward the Mississippi River.

Because of its gentle channel slope and sluggish currents, the Big Muddy rises slowly and stays in flood for relatively long periods (US Army Corps of Engineers, 1968). Flooding on the main stem of the river is currently monitored by nine stream gages. The nearest stream gage to the study site is located 10 km upstream, at Murphysboro.

There are twelve reservoirs of varied capacity in the Big Muddy River drainage basin, the largest of which is Rend Lake. The Rend Lake reservoir and dam, completed in October 1970, lies at the northern end of the watershed. It was designed to reduce downstream flooding by 35% (U.S. Army Engineer District, 1970). Since construction of the lake, mean discharge at Murphysboro has been reduced by 5% (USGS, 1991). The remainder of the reservoirs are intended for recreational and water supply use, and provide only limited flood control (USACOE, 1968; USAED, 1970).

2.B Geology and Geomorphology

The Big Muddy basin lies between a large sandstone and limestone cuesta to the east and the Ozark Plateau to the west (Harris, et al., 1977). The Shawnee Hills region is a complex, dissected upland located south of past glaciation limits (USACOE, 1968). Glacial outwash on the Mississippi River channel created a broad, thick floodplain which encompasses the lower 70 km of the Big Muddy River (USAED, 1970). Bottomland soils are mainly silt, clay, and loess, with poor drainage (US Department of Agriculture, 1975).

During flooding, sediment is carried out of river channels and onto the floodplain. Coarse material is often deposited near the bank, building natural levees (Harris, et al., 1977). The active Big Muddy floodplain is not very flat as it contains overflow scour channels and raised bars. Older, higher levels are rarely flooded, while lower surfaces are more frequently scoured. Terraces, at the highest level above the flat floodplain, are themselves remnants of an abandoned floodplain (Harris, et al., 1977).

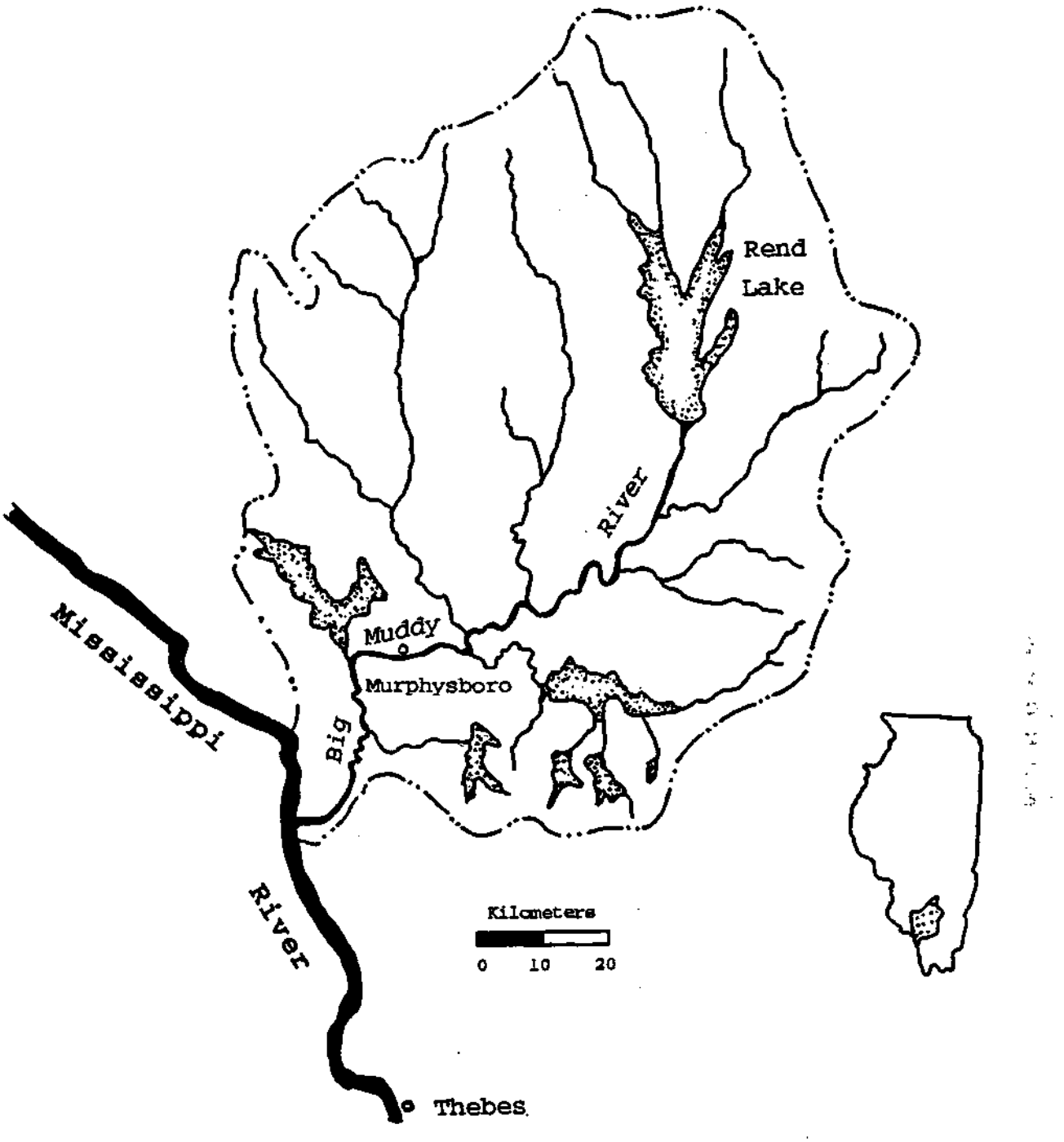

Figure 5. Big Muddy River drainage basin in southern Illinois.

2.C Climate and vegetation

The climate of the lower Big Muddy River basin is characterized by hot and humid summers, and relatively mild winters (Table 1). Mean annual precipitation is 111.2 cm, with a peak during the spring. The growing season for the study section of the river lasts about 200 days, from mid-April to late October (USACOE, 1968). Summer precipitation is generally discontinuous in the form of rainshowers, while winter precipitation is more uniformly distributed across the region. Winter precipitation, infrequently snow, results in a good accumulation of soil moisture by spring and minimizes drought during summer on most soils in most years (Herman, 1979).

Table 1. Climate data for Carbondale. Illinois. Data listed are: 1961-1991 mean monthly values of maximum temperature, minimum temperature, and precipitation (from Illinois State Water Survey).

	Jan	Feb	Mar	Apr	May	Jun
Mean max T (C)	4	7	13	20	26	30
Mean min T (C)	-1	2	8	14	19	23
Mean P (mm)	66	74	117	102	114	107
	Jul	Aug	Sep	Oct	Nov	Dec
Mean max T (C)	32	31	27	21	14	7
Mean min T (C)	26	24	21	14	8	2
Mean P (mm)	94	102	76	64	99	97

Vegetation in the Shawnee Hills is topographically graded from bottomland to ridge crest. Hillslopes and ridges are dominated by short grasses and several species of oak, while bottomlands have a great variety of flora to include cottonwood, maple, elm, and oak (USACOE, 1968).

2.D Field site description

The field site for this research is on floodplain and uplands east of the Dillon Bend meander of the Big Muddy River, 12 km upstream from its confluence with the Mississippi (Figure 6). Dillon Bend is bordered by 100 m bluffs to the east and abandoned Mississippi River floodplain to the west. The location of the study site is remote, accessible by unimproved road at the base of the bluffs along which there are no habitations or permanent structures. Land surrounding Dillon Bend is devoted mainly to national forest, although there are a few small agricultural plots nearby. A levee parallels the river about 2 km west of Dillon Bend (Figure 7). The levee, part of the Grand Tower Drainage and Levee District, was completed in 1959 to protect residents and agricultural land from high flows on the Big Muddy and Mississippi (Dobney, 1975).

The landscape at the Dillon Bend study site has a definite lower floodplain level interrupted by higher banks and natural levees. The banks and levees vary in width; 5-10 m in some spots while spanning broad fields in other locations. If the banks are remnant terraces or ancient river sediments, some soil development would most likely have occurred (Johnson, personal communication, 1992; Martin, 1992). A natural cutbank exposure cut into the fill of a terrace was examined for soil development. The top of the cutbank is about 4 m above the bankfull level of the Big Muddy River. The bank contains unstratified fill with signs of leaching, but with no visible sign of a clay (B) horizon. This suggests that the highest surface on the eastern side of Dillon Bend is relatively young and aggrading, and most likely a historically active floodplain.

2.E Known flood history

The floodplain along the Dillon Bend section of the Big Muddy River is prone to flooding under two separate scenarios. The first situation involves flows resulting from runoff within the Big Muddy drainage basin, and is characterized by high gaged discharge at the Murphysboro stream gage. Secondly, high flows on the Mississippi River may result in backwater flooding of the lower 60 to 80 km of the Big Muddy, which includes Dillon Bend (USAED, 1970). The nearest streamgage to the Big Muddy/Mississippi River confluence is at Thebes, Illinois, 51 km downstream from Dillon Bend.

The occurrence and degree of flood events is best measured with values of peak stage, or the maximum height of floodwaters at a gaging station. The known flood history, with related stages, for the lower Big Muddy River from gaged records and historical data can be summarized as follows:

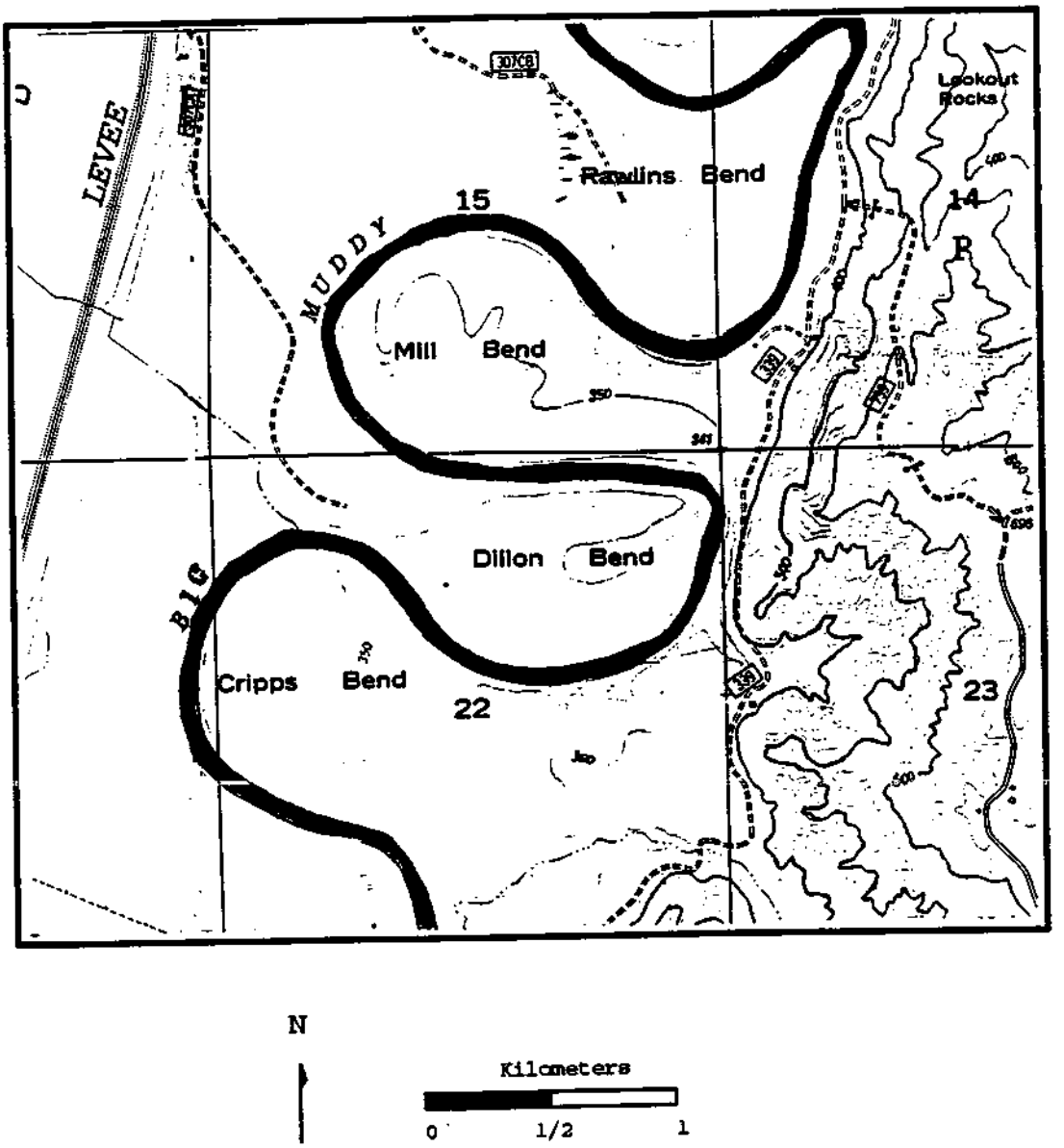

Figure 6. Dillon Bend section of the Big Muddy River (after USGS, 1990).

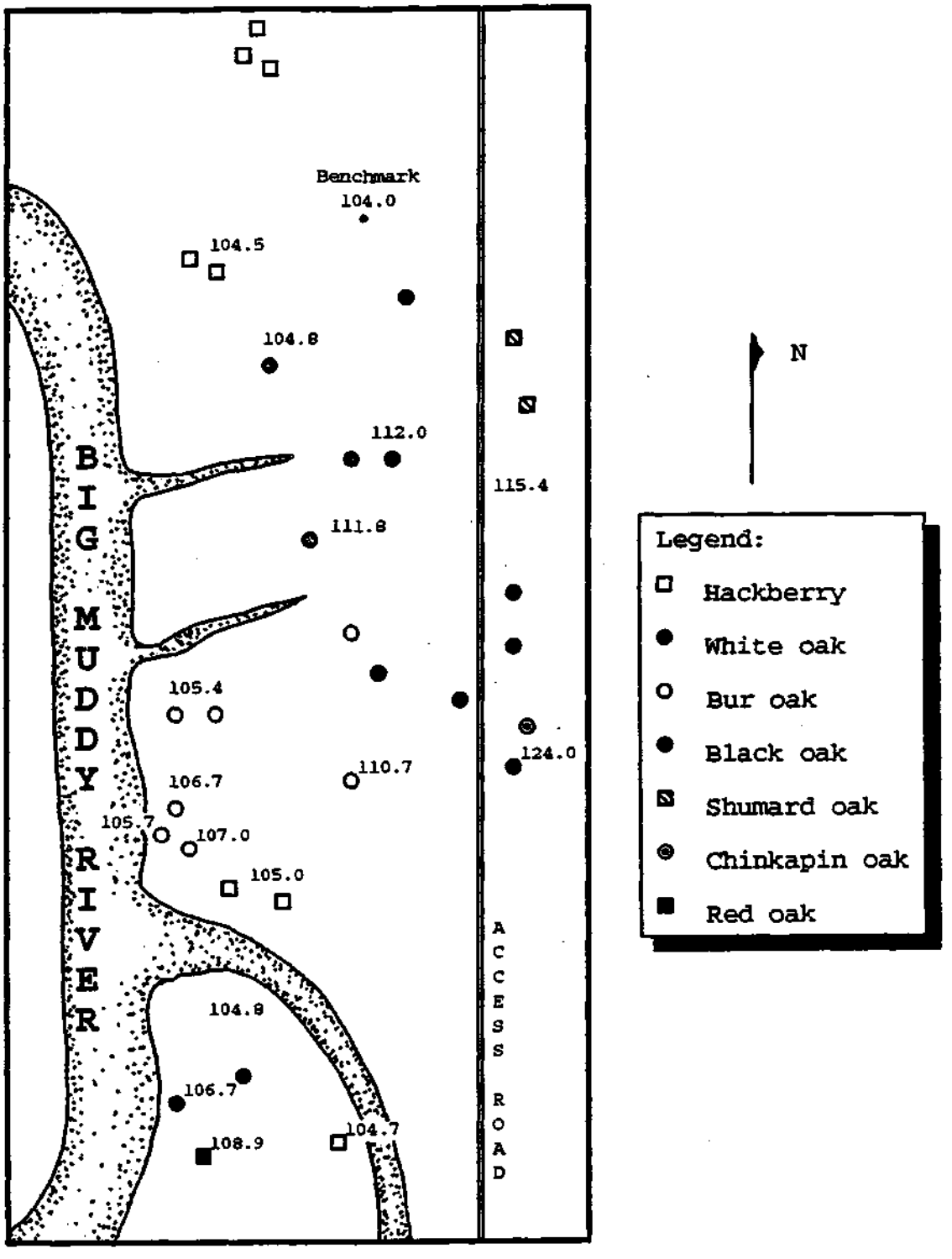

Figure 7. Distribution of trees sampled along the Dillon Bend reach of the Big Muddy River. Horizontal distances are not to scale. Spot elevations represent surveyed ground level in meters above sea level (MSL).

2.E.1 Flooding from high flow of the Big Muddy River

There have been numerous historical reports of damaging floods in the Big Muddy River basin since the early 1900s. "Newsworthy" flood events were all associated with peak stages of at least 10.0 m at the Murphysboro gage (USACOE, 1968; USAED, 1970). The Murphysboro gage has been recording river stage since 1916, but data is fragmentary prior to 1931. Significant flooding was reported by area residents in March 1913 and August 1915, but nothing is known about the magnitudes of these events.

From 1916 to present, the reported stage at Murphysboro has reached 10.0 m or greater 11 times (Table 2). The flood of record occurred on May 12, 1961, when the stage peaked at 11.6 m. A major storm over the basin had produced widespread rain and the record discharge for all gaging stations on the main stem (USACOE, 1968). Relative magnitudes of other gaged flood events are compared with values of peak stage in Table 2.

2.E.2 Backwater flooding from the Mississippi River

Comparison of gaged records between Murphysboro and Thebes shows that high stages usually do not occur simultaneously at the two locations. Thebes discharge includes inputs from the entire Upper Mississippi River watershed (1,847,188 km^2), while flow at Murphysboro responds to runoff from its own, much smaller watershed (5,618 km^2). Major floods on the Upper Mississippi River usually occur between March and June, from rapid melting of a large accumulation of snow (USAED, 1970). Considering that weather systems and climatic conditions that contribute to runoff and snowmeit vary dramatically over such a large area, and that there is a significant lag time for Thebes discharge to respond to runoff inputs, it is not surprising that peak stages between Thebes and Murphysboro are not coincident.

The streamgage at Thebes has been recording discharge data since 1934, but stage measurements from an auxiliary gage 13 km upstream date back to 1896. The only known major flood outside the period of record occurred in July, 1844, with an estimated stage of 13.0 m, computed by the U.S. Army Corps of Engineers using floodmarks (USGS, 1991). The Mississippi River floods of 1943, 1944, and 1947 are documented to have caused backwater flooding on the lower section of the Big Muddy River, contributing to the high stages recorded at Murphysboro for those years (USACOE, 1968). A farmer who currently manages fields along the eastern bank of the Big Muddy south of Dillon Bend, confirmed that the area is highly prone to backflooding from the Mississippi River. The backwaters are said to overflow the banks near Dillon Bend when the stage at the Thebes streamgage measures about 9.7 m (Dennis Ballance, personal communication, 1992).

Table 2. Stage data for major floods (greater than 10.0 m) in the Big Muddy River basin, recorded at the Murphysboro gaging station (from USACOE, 1968; United States Geological Survey, 1991).

Flood	Peak Stage at Murphysboro (m)
May 1933	10.3
March 1935	10.4
January 1937	10.3
August 1946	10.1
January 1949	11.0
January 1950	10.8
April 1957	10.3
May 1961	11.6
March 1979	10.4
May 1983	11.2
April 1985	10.2

Since 1932, the stage of the Mississippi River at Thebes has exceeded 9.7 m 47 times in 45 years. Peak stage on record at Thebes occurred with the April 1973 flood, when the floodwaters reached 13.2 m. The rare event occurred as the Mississippi, Missouri, and Illinois Rivers crested simultaneously (Dobney, 1978). This and other floods are compared in Table 3.

Table 3. Stage data for major floods on the Upper Mississippi River, recorded at the Thebes gaging station (from USACOE, 1945; USGS, 1993).

Flood-Stage Data for Thebes, Illinois			
Flood	Peak State (m)	Flood	Peak Stage (m)
July 1844	13.0"	July 1951	12.1
June 1903	11.1	May 1952	11.1
May 1904	10.4	July 1958	10.3
June 1908	10.4	April 1960	11.3
July 1909	10.6	May 1961	11.8
April 1912	10.6	March 1962	11.0
August 1915	10.4	April 1965	10.4
February 1916	11.1	October 1966	9.9
June 1916	11.1	July 1969	11.8
April 1920	9.8	May 1970	11.0
April 1922	11.6	March 1971	10.0
October 1926	10.0	April 1972	10.0
April 1927	12.2	April 1973	13.2
June 1928	10.0	May 1974	10.0
May 1929	11.4	April 1975	11.0
May 1933	10.5	March 1978	11.6
June 1935	11.1	April 1979	13.1
June 1942	10.8	May 1983	12.1
May 1943	12.2	April 1984	11.7
May 1944	11.9	March 1985	12.3
April 1945	11.5	November 1985	12.3
January 1946	10.2	October 1986	12.6
July 1947	12.2	Mar 1990	12.1
May 1950	9.8		

*estimated from floodmarks

CHAPTER 3
METHODS

3.A Data acquisition and analysis

3.A.1 Tree cores

Coring procedures:

Objectives at the research site were to sample trees of a favorable species and longevity for dendroclimatic research, and to core several levels above the floodplain on the hillslope and terrace. U.S. Forest Service personnel, Harrisburg office, provided assistance in locating old tree stands. Oak and hackberry were sampled due to their abundance, longevity, and proven response to hydrologic stimuli (Hosner and Boyce, 1962). Collected species include black oak (Quercus velutina Lam.), white oak (Quercus alba L.), bur oak (Quercus macrocarpa Michx.), chinakpin oak (Quercus meuhlenbergii Engelm.), shumard oak (Quercus shumardii Buckl.), red oak (Quercus Rubra L.), and hackberry (Celtis occidentalis Torr.). Minimum sample size at each elevational level was five trees for chronology development. Sampling distribution is shown in Figure 7.

At least two cores per tree, separated by 90° , were extracted to account for variable and irregular growth patterns within the stem (Stokes and Smiley, 1968). Parts of the stem where rings might be distorted (such as uphill/downhill sides and parts near branches) were not sampled. Cores were directed toward the pith to obtain a full record of the tree's longevity.

Tree cores were taken with a Haglof 4.3 mm increment borer, which screws into the tree and removes a cylindrical sample in which the rings are preserved. Cores were removed from the borer and placed in plastic straws, sealed and numbered. Notes were taken on location, species, elevation above the river, core orientation, and physical condition of the tree (Stokes and Smiley, 1968). Each sampled tree was labeled with a metal tag.

Ring measurement:

Cores were allowed to dry for a few days in the straws to prevent warping. They were then mounted on pine strips and sanded with medium grade sandpaper to give a flat, measurable surface. Sanded surfaces were shaved using a razorblade to expose cells, and given a final sanding with 400 grade sandpaper. After the rings were counted and marked by decades, the width of each annual ring was measured and recorded using a stage microscope. For consistent methodology, all measurements were made perpendicularly across rings from latewood to earlywood boundaries so that the relative ring widths could be compared (Stokes and Smiley, 1968).

Flood ring identification:

Low level (floodplain) and mid-level cores were inspected under a microscope for wood abnormalities related to flooding. Flood rings were identified and annotated for growth year and intra-ring position of the abnormal growth (i.e. mid-latewood). Ring position can be used to estimate the relative time of flooding during the growing season. After inspection of cores was completed, flood ring years were marked on a time chart with separate time lines for each tree, so that commonalities could be identified.

3.A.2 Hydrologic data

Stream gage records provide mean daily discharge data (cubic meters per second) and extreme peak discharges (m^3/s) for the duration of a station's operation. Mean monthly discharge data from two gages were collected with assistance from personnel at United States Geological Survey, Urbana office. Gages at Thebes and Murphysboro were selected for proximity to the study site and length of record. The Thebes gage monitors the Mississippi River 51 km downstream from the Mississippi/Big Muddy confluence, recording from 1934 to present. The Murphysboro gage is located on the Big Muddy River 10 km upstream from Dillon Bend, and has been operating since 1916 (fragmentary prior to 1931)(USGS, 1991).

3.A.3 Climate data

The National Weather Service maintains daily records of temperature and precipitation for some 200 locations in Illinois. For this study, average maximum temperature and precipitation totals for Carbondale and Anna were collected for each month of each year since 1901. The data can be used to determine the effect of temperature and precipitation on tree growth during the growing season, and during the spring months when growth begins. Precipitation during the fall and winter months prior to the next growing season can be used to study the influence of soil moisture storage.

3.B Model development

3.B.1 Crossdating

Before continuing with model development, it is necessary to accurately date the rings within the tree cores. This includes accounting for missing rings at the ends of or within the cores, and multiple or false rings. Since trees record the environment in a pattern of wide and narrow rings, it is possible to match patterns, or crossdate trees (Fritts, 1976). The calendar year of the outermost ring, known when bark is present, serves as the starting point for crossdating.

The procedure of crossdating uses the COFECHA computer program (see Appendix B), which aids in identifying errors and acts as an independent tool to confirm the accuracy of dating and measurement (Holmes, et al., 1986). The dated and measured ring series are filtered by fitting a 20-year cubic spline, and then dividing the series values by the corresponding spline curve values to remove low-frequency variance. The high frequency residual is subjected to a log transformation to equalize proportionally the variability among small and large rings (Holmes, et al., 1986). The mean values of the combined series comprise the master dating chronology. After an initial COFECHA run using the 40 oak ring series, the 10 series with the best correlation to the master are selected to compose a more reliable master dating chronology. Each COFECHA output identifies measuring or counting errors by flagging 40 year ring segments and individual outliers within each core that do not agree with the master. After using the output to account for possible problems in master cores, each of the remaining cores are added one by one to the COFECHA program and checked against the master chronology. As measuring or counting errors are remedied, each core is included in the final dating chronology.

3.B.2 Standardization

Ring-widths generally decrease as trees age, due to the tree's ever-increasing diameter (Fritts, 1976). To compare trees with different growth rates and ages, growth trend analysis procedures must be used to produce annual standardized, dimensionless indices for all rings. The computer program ARSTAN (see Appendix B) fits either negative exponential curves or stiff cubic splines to tree-ring series (Holmes, et al., 1986). Trend curves differ in form depending upon site-specific growth variations and distance from the pith of the tree. Visual inspection of raw ring-widths is used to estimate whether the trend of growth is a clear departure from negative exponential. ARSTAN prompts as to whether the operator believes there are any cores with clear departures. Specified cores are fitted with cubic splines to model growth trend. Figures 8-10 show raw ring-widths plotted against their computer-fitted growth curves. Note that cores DB37, DB38, and DB43 did not have negative exponential growth trends, requiring cubic spline treatment.

An annual index is computed by dividing the measured ring width by the value of the growth curve for that particular year. To account for the lag influence of previous years' growth, ARSTAN uses autoregressive modeling to enhance the common signal (Holmes, et al., 1986). The chronology of a tree core is then expressed as a series of indices that are stationary in both mean and variance (Stockton, 1975).

Master chronologies are constructed for the floodplain, mid-slope, and high level trees by combining the indices from individual cores from each level, and computing an average growth index for each year in the combined chronology. Each of the three levels are then represented by a single master chronology.

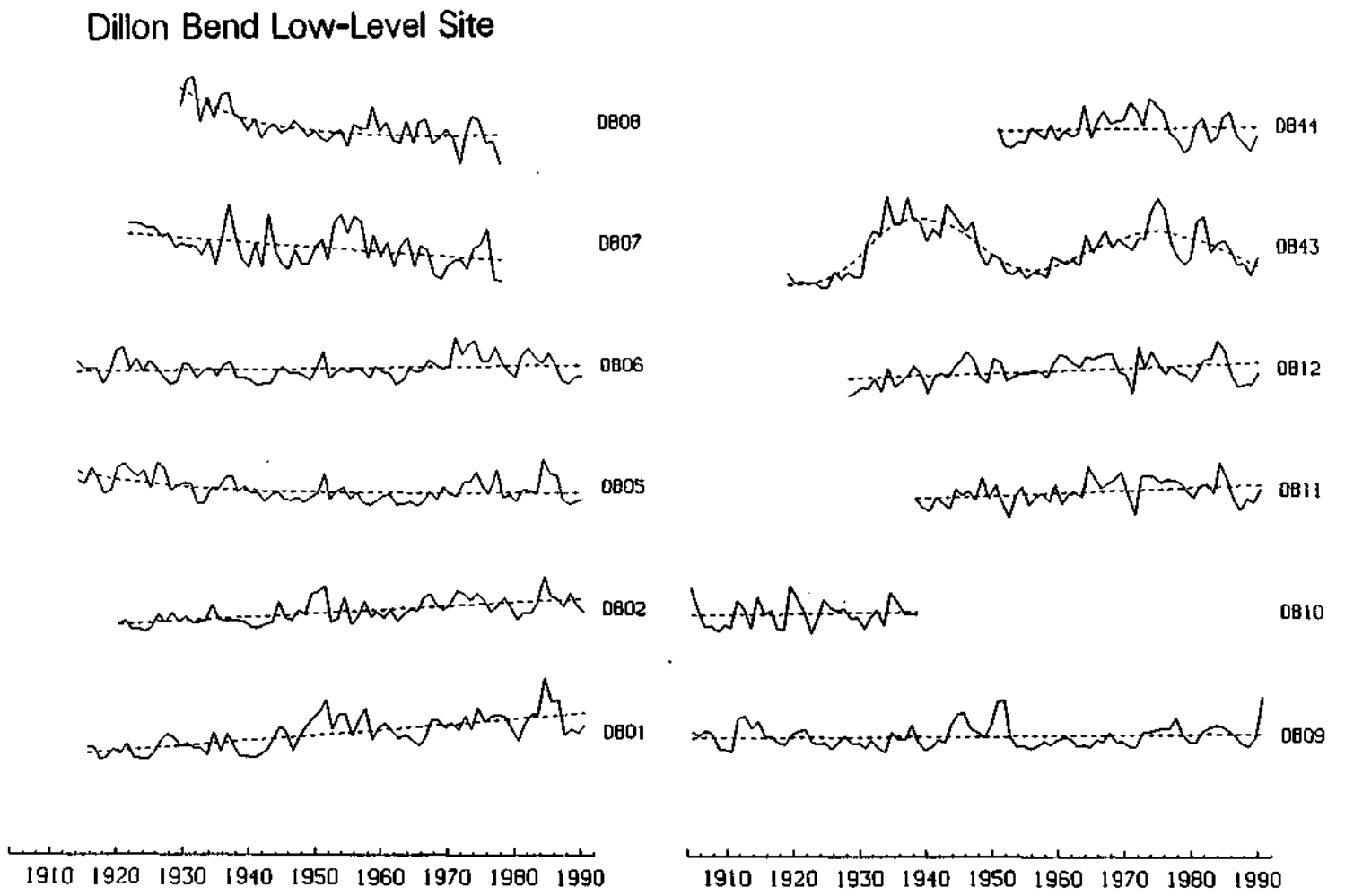

Figure 8. Raw ring-widths from low-level (floodplain) trees fitted with growth trend curves using the computer program ARSTAN. Core species are bur oak, except for DB44 and DB43, which are white oak.

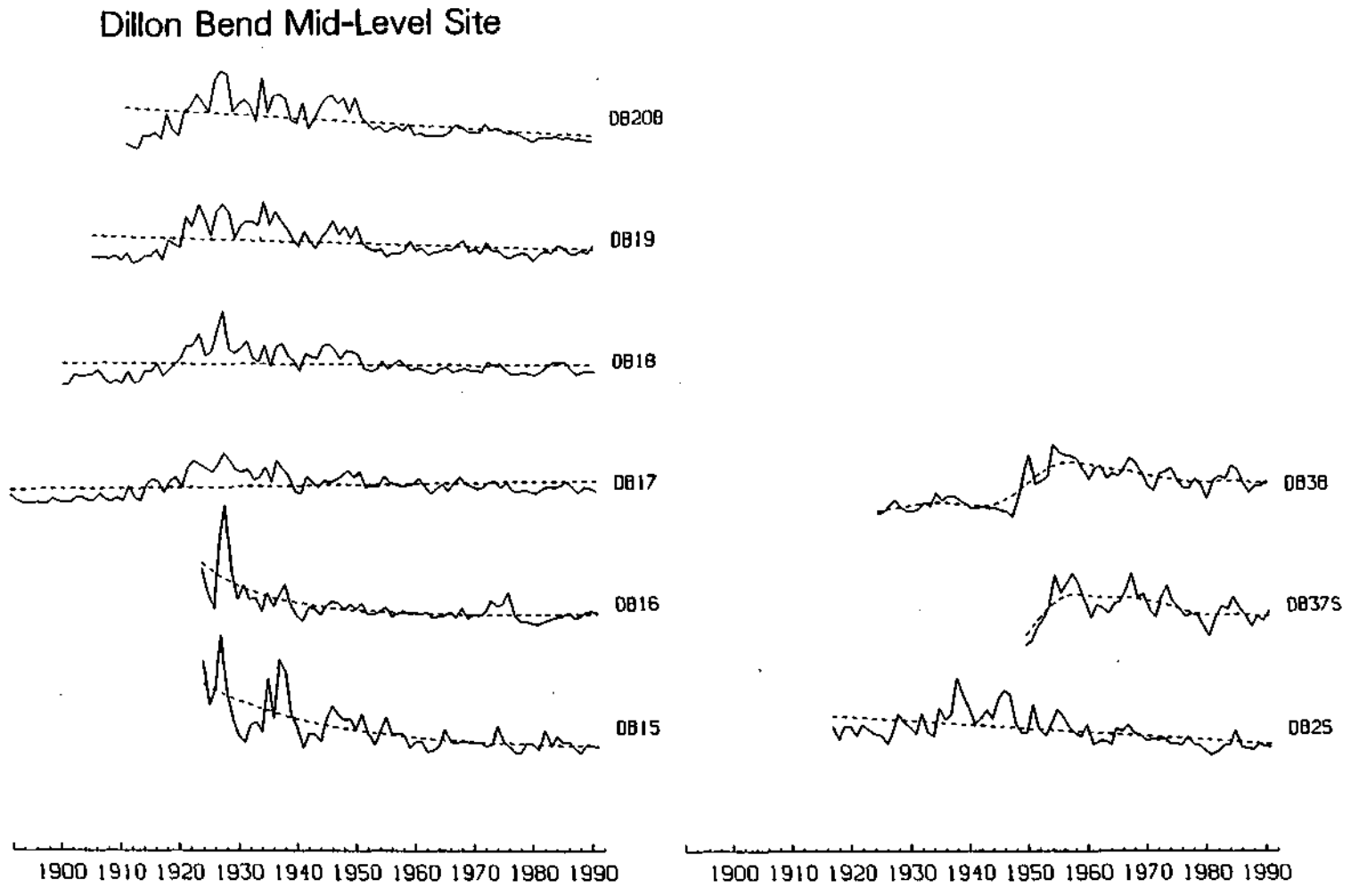

Figure 9. Raw ring-widths from mid-level trees fitted with growth trend curves using the computer program ARSTAN. Core species for DB15 through DB20 are white oak. DB37 and DB38 are black oak. DB25 is bur oak.

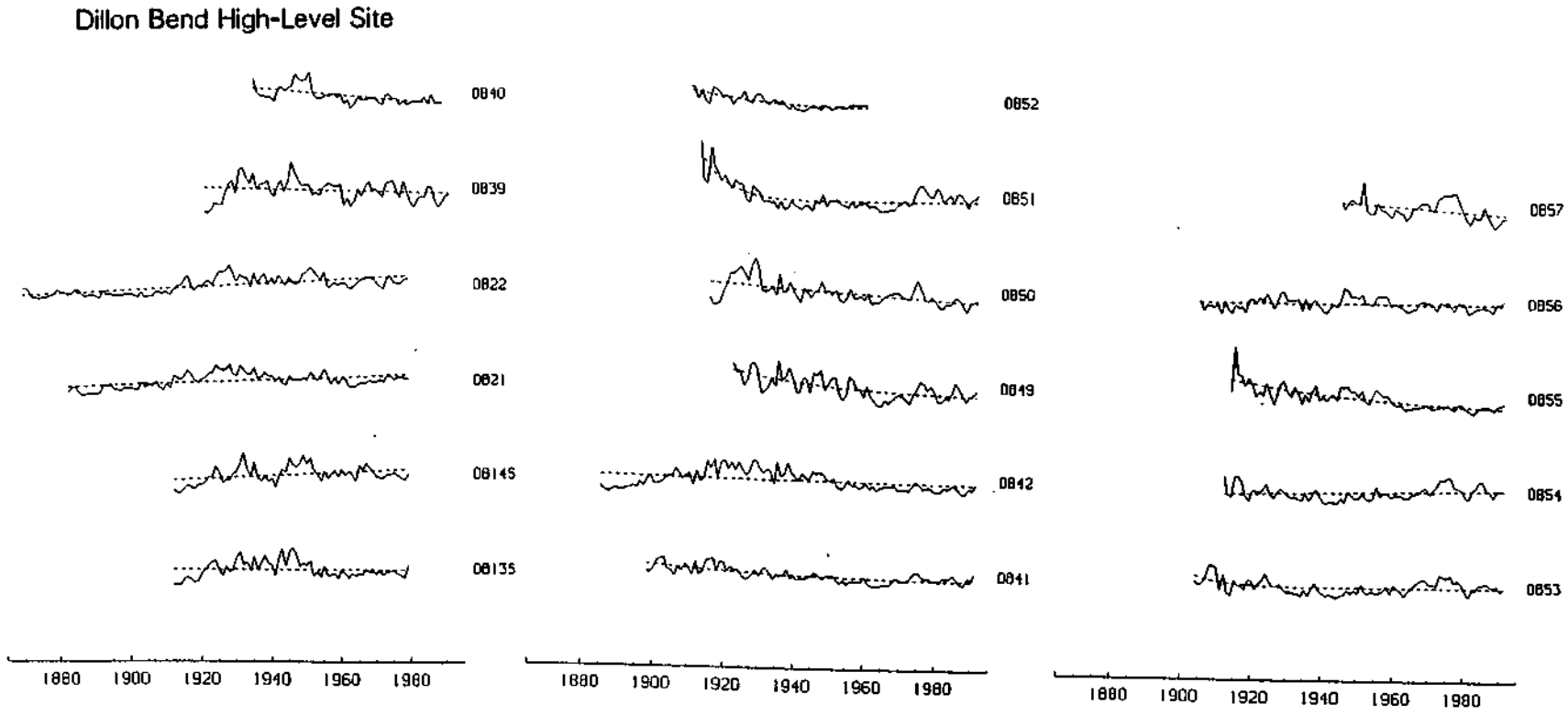

Figure 10. Raw ring-widths from high-level trees fitted with growth trend curves using the computer program ARSTAN. Core species are black oak: DB39, DB40, DB49, DB50, DB53, DB54; bur oak: DB14, DB14; chinkapin oak: DB51, DB52; white oak: DB21, DB22, DB41, DB42; Shumard oak: DB55, DB56, DB57.

3.B.3 Correlation analysis

Paleoflood analysis requires testing of the relationship between tree-ring growth, climate, and discharge. Prior to a regression analysis, it is necessary to measure correlation between these variables, so that significant months or seasons (groupings of months) can be identified. Pearson correlation coefficients with a 95% level of confidence are identified between environmental variables and the following growth variables: floodplain trees, mid-slope trees, high level trees, and ratios of floodplain/high trees. Coefficients are calculated for all 12 months of the growth year, and May through December of the previous year to account for lag effects. With tree growth as the dependent variable, independent variables were selected for the following reasons:

a. Carbondale monthly precipitation and temperature
   Determines the degree of a linear relationship between tree-growth and local precipitation and temperature recorded at the nearest climate station within the Big Muddy watershed.

b. Anna monthly precipitation and temperature
   Determines the degree of a linear relationship between tree-growth and local precipitation and temperature recorded at the nearest weather station in an adjacent watershed.

c. Regional precipitation and temperature for Illinois Climate Division 8.
   Determines the degree of a linear relationship between tree-growth and precipitation and temperature from the lower section of the Upper Mississippi watershed above the Mississippi-Ohio River confluence.

d. Illinois regional Palmer Drought Severity Index (PDSI).
   Determines the degree of a linear relationship between tree growth and drought as defined by PDSI (see Appendix A).

e. Illinois regional Palmer Hydrologic Drought Index (PHDI).
   Determines the degree of a linear relationship between tree growth and soil moisture as defined by PHDI (see Appendix A).

f. Murphysboro mean monthly discharge.
   Determines the degree of a linear relationship between tree-growth and flow from the Big Muddy River watershed.

g. Thebes mean monthly discharge.
   Determines the degree of a linear relationship between tree growth and flow from the Mississippi River watershed north of Thebes (known to backflood the Big Muddy channel).

After correlations are calculated for each of these monthly variables, relationships which are significant at the 0.05 level are identified. Consecutive significant months are grouped into "seasons", and correlations between these aggregate variables and tree-ring growth are calculated. Further statistical analysis uses the seasonal variables with the highest correlations, provided that they are reasonable environmental parameters.

3.B.4. Comparisons

To investigate the effects of flooding on floodplain trees compared to upland trees, ratios of floodplain/upland standardized ring-width indices are computed for each year of the tree-ring chronology (see 1.D.3). The ratios are first plotted against normalized seasonal discharge data to identify how well trends in tree-ring ratios conform to trends in discharge. Then, the best-correlated discharge variable (determined from correlation analysis) is regressed on the ratio variable to develop a predictive model for flood reconstruction.

3.B.5 Bivariate linear regression

Since the nature of this research is flood reconstruction, it is necessary to analyze the relationship between discharge and tree-ring growth. This is accomplished by regressing discharge on the standardized chronologies, where discharge variables are the seasonal totals selected from correlation analysis. One half of the discharge data set is used for model calibration, and the other saved for verification of the derived model. The SAS statistical software package is used to compute model parameters and analysis of variance (ANOVA) test statistics. The regression equation is verified against the remaining half data set using the VERIFY software package (see Appendix B) (Holmes, et al., 1986). Verification results are tested at the 95% confidence level for correlation, reduction of error, and T-value.

CHAPTER 4
RESULTS

4.A Chronology development

Two of the most important procedures in chronology development are crossdating and standardization. Crossdating assures proper placement in time of each annual ring, and standardization corrects for systematic growth changes resulting from tree aging (Fritts, 1976). Separate chronologies were developed for the floodplain, mid-slope and high level collection sites at Dillon Bend. Specifics on chronology development are explained in this section.

4.A.1 Crossdating and verification

The final floodplain, mid-slope and high level data sets consist of 12, 9, and 17 cores, respectively. The computer program COFECHA (Holmes, et al., 1986) was used to identify and correct possible dating or measurement errors in the 38 cores (see Appendix B). A total of 4 cores were omitted from the data set because of poor correlation with the master series for their respective site. Three of the 4 abandoned cores were from the floodplain site, which has the most variable growth regime due to differential drainage from uneven topography.

The minimum acceptable correlation coefficient in crossdating was 0.3665, which represents a 99% level of confidence when testing 40 year segments of the cores. A segment length of 40 years provided sufficient degrees of freedom to avoid chance correlations, while being short enough to help locate dating problems (Holmes, et al., 1986). Descriptive statistics ,, on the final chronology for each site are listed in Tables 4-6.

DILLON BEND FLOODPLAIN TREES

Number of dated series: 12
Master series 1905-1991: 87 yrs
Average mean sensitivity: .221
Series intercorrelation: .538

Series	Interval	#Years	#Flags	Corr. w/ Master
DB01	1916-1991	76	0	.588
DB02	1921-1991	71	0	.524
DB05	1915-1991	77	1	.539
DB06	1915-1991	77	0	.552
DB07	1923-1979	57	0	.481
DB08	1931-1979	49	0	.473
DB09	1905-1991	87	0	.605
DB10	1905-1939	35	0	.585
DB11	1939-1991	53	0	.466
DB12	1929-1991	63	0	.494
DB43	1920-1991	72	0	.530
DB44	1952-1991	40	0	.589
			Mean:	.538

Table 4. Descriptive statistics on floodplain tree cores after completion of crossdating procedures. # Flags refers to the number of 40 year segments which had less than .3665 correlation with the master floodplain chronology. The overall series correlation with the floodplain master is listed in the final column.

DILLON BEND MID-SLOPE TREES

Number of dated series: 9
Master series 1892-1991: 100 yrs
Average mean sensitivity: .239
Series intercorrelation: .664

Series	Interval	#Years	#Flags	Corr. w/ Master
DB15	1924-1991	68	0	.597
DB16	1924-1991	68	0	.630
DB17	1892-1991	100	0	.711
DB18	1901-1991	91	0	.721
DB19	1906-1991	86	0	.720
DB20	1912-1991	80	0	.737
DB25	1917-1991	75	1	.530
DB37	1950-1991	42	0	.663
DB38	1925-1991	67	1	.617
				Mean: .664

Table 5. Descriptive statistics on mid-slope tree cores after completion of crossdating procedures. # Flags refers to the number of 40 year segments which had less than .3665 correlation with the master mid-slope chronology. The overall series correlation with the mid-slope master is listed in the final column.

DILLON BEND HIGH ELEVATION TREES

Number of dated series: 17
Master series 1905-1991: 123 yrs
Average mean sensitivity: .220
Series intercorrelation: .643

Series	Interval	#Years	#Flags	Corr. w/ Master
DB13	1912-1979	68	0	.552
DB14	1912-1979	68	0	.623
DB21	1882-1979	98	0	.510
DB22	1869-1979	111	1	.514
DB39	1921-1991	71	0	.643
DB40	1935-1989	55	0	.547
DB41	1898-1991	94	0	.610
DB42	1885-1939	107	0	.666
DB49	1922-1991	70	0	.676
DB50	1915-1991	77	0	.762
DB51	1912-1991	80	0	.694
DB52	1909-1959	51	0	.607
DB53	1904-1991	88	0	.685
DB54	1912-1991	80	0	.720
DB55	1914-1991	78	0	.631
DB56	1905-1991	87	0	.799
DB57	1945-1991	47	0	.718
				Mean: .643

Table 6. Descriptive statistics on high-level tree cores after completion of crossdating procedures. # Flags refers to the number of 40 year segments which had less than 0.3665 correlation with the master high-level chronology. The overall series correlation with the high-level master is listed in the final column.

The mean correlation coefficients for the floodplain (0.538), mid-slope (0.664), and high sites (0.643) are very good for a deciduous species such as oak (Estes, 1970; Henri Grissino-Mayer, personal communication, 1992). It is not surprising that the mid-slope and high sites have higher mean correlations than the floodplain site, since their climate sensitive landscape position favors a common response among trees.

Another important computed statistic is mean sensitivity, which is a measure of change in ring width from one year to the next. The average mean sensitivity in many dendrochronologic studies is 0.35, with a 99% confidence interval of 0.13 to 0.57 (Fritts, 1991). The Dillon Bend chronologies have mean sensitivities ranging from 0.220 to 0.239, well within common limits. The value of 0.221 for the floodplain site was surprisingly high when considering its poor drainage and abundant moisture supply. This unexpected result may reflect the fact that the floodplain is uneven, with banks and scour holes which vary the relief, drainage pattern, and effects of floodwaters.

Before finalizing a chronology, it is standard practice to verify core measurement and dating by having a second party remeasure 10% of the cores which compose a chronology (Fritts, 1976). Henri Grissino-Mayer from the Laboratory of Tree-Ring Research at the University of Arizona randomly selected 4 of the 38 oak cores and remeasured them using equipment at the University of Arizona, Tucson. He verified his measurements against my own using the MEASURE computer program (see Appendix B). Inspection of descriptive statistics (average ring width, standard deviation, etc.) for the original and remeasured cores suggests an accurate measurement, which was then confirmed by a Matched Pairs difference of means test at the 95% level of confidence (see Tables 7-10).

VERIFICATION RESULTS

Core selected: DB01

Descriptive statistics

	Original file	Verification file
Average width (mm)	4.027	4.028
Median (mm)	3.990	3.975
Variance	1.956	1.992
Std. deviation (mm)	1.399	1.411
Coef. variation	0.347	0.350
Mean sensitivity	0.205	0.192
Autocorrelation	0.746	0.766

Regression results

Dependent variable (y)	original DB01 file
Independent variable (x)	verification file
Slope of regression	0.984
Intercept of regression (mm)	0.064
Coefficient of variation	4.165
Correlation coefficient	0.993

Verification results: 1916-1991

	Test for Matched Pairs
Sum of differences	9.200
Total square differences	2.121
Avg absolute differences	0.121
Mean square differences	0.028
Test statistic *t*	1.043

Accepted at 95% level of confidence

Table 7. Output statistics from the computer program MEASURE, which compares two independent measurements of core DB01.

VERIFICATION RESULTS

Core selected: DB08

Descriptive statistics

	Original file	Verification file
Average width (mm)	4.321	4.321
Median (mm)	4.470	4.400
Variance	2.942	2.973
Std. deviation (mm)	1.715	1.724
Coef. variation	0.397	0.399
Mean sensitivity	0.243	0.237
Autocorrelation	0.750	0.750

Regression results

Dependent variable (y)	original DB08 file
Independent variable (x)	verification file
Slope of regression	0.991
Intercept of regression (mm)	0.038
Coefficient of variation	3.426
Correlation coefficient	0.996

Verification results: 1931-1989

	Test for Matched Pairs
Sum of differences	6.230
Total square differences	1.263
Avg absolute differences	0.106
Mean square differences	0.021
Test statistic *t*	1.060

Accepted at 95% level of confidence

Table 8. Output statistics from the computer program MEASURE, which compares two independent measurements of core DB08.

VERIFICATION RESULTS

Core selected: DB21

Descriptive statistics

	Original file	Verification file
Average width (mm)	1.979	1.979
Median (mm)	2.040	2.115
Variance	0.540	0.557
Std. deviation (mm)	0.735	0.747
Coef. variation	0.371	0.377
Mean sensitivity	0.190	0.208
Autocorrelation	0.803	0.788

Regression results

Dependent variable (y)	original DB21 file
Independent variable (x)	verification file
Slope of regression	0.961
Intercept of regression (mm)	0.077
Coefficient of variation	7.937
Correlation coefficient	0.977

Verification results: 1882-1991

Test for Matched Pairs

Sum of differences	10.990
Total square differences	2.755
Avg absolute differences	0.100
Mean square differences	0.025
Test statistic *t*	0.997

Accepted at 95% level of confidence

Table 9. Output statistics from the computer program MEASURE, which compares two independent measurements of core DB21.

VERIFICATION RESULTS

Core selected: DB38

Descriptive statistics

	Original file	Verification file
Average width (mm)	3.281	3.279
Median (mm)	3.350	3.310
Variance	2.236	2.353
Std. deviation (mm)	1.495	1.534
Coef. variation	0.456	0.468
Mean sensitivity	0.200	0.215
Autocorrelation	0.856	0.843

Regression results

Dependent variable (y)	original DB38 file
Independent variable (x)	verification file
Slope of regression	0.972
Intercept of regression (mm)	0.095
Coefficient of variation	3.629
Correlation coefficient	0.997

Verification results: 1925-1991

Test for Matched Pairs

Sum of differences	6.500
Total square differences	1.046
Avg absolute differences	0.097
Mean square differences	0.016
Test statistic *t*	1.201

Accepted at 95% level of confidence

Table 10. Output statistics from the computer program MEASURE, which compares two independent measurements of core DB38.

4.A.2 Standardization

A standardized master chronology was computed for the floodplain, mid-slope and high collection levels using the ARSTAN computer program (see Appendix B). Ring width data for all cores were entered into the program, which applied growth trend analysis and autoregressive modeling to produce a standardized index value for each year at each of the collection levels (Holmes, et al., 1986). The mean value of the indices for each chronology approximated 1.0, allowing data from trees with different growth rates to be combined or compared for climatic variation. Standardized indices for each chronology are shown in Figure 11 and numerical values are listed in Appendix D.

Verification of a regional climatic signal was accomplished by comparing standardized indices of the Dillon Bend high elevation cores with those from 2 nearby sites, as suggested by Fritts (1991), Kutzbach and Guetter (1980), and Estes (1970). The nearest tree-ring study to the Dillon Bend area was that of Estes, in the Pine Hills area east of the Big Muddy River, about 11 km south of Dillon Bend. He sampled shortleaf pine for correlation with precipitation data. Biasing and Duvick (1984) collected cores for precipitation reconstruction from white oak at Giant City State Park, Illinois, which is about 20 km from the Dillon Bend site. Resulting ring-with indices from these two studies, available from the International Tree-Ring Data Bank (ITRDB), were plotted against the Dillon Bend high oak chronology (Figure 12). The major wet/dry trends in the shortleaf pine chronology are similar to that of Dillon bend oak, although there are dramatic departures in amplitude for some years. A one-year lag appears in the final 10 years of the shortleaf pine chronology, which may be due to species-related differences or a missing ring in the pine chronology, which often occurs with moisture stressed conifers (Fritts, 1976). Some agreement between the oak chronologies of Giant City and Dillon Bend is evident, indicating a reflection of a common climatic signal.

An appearance of correlation between separate study sites is encouraging, but most critical to tree-ring studies is the measure of correlation between growth indices and environmental variables.

4.B Correlation with environmental variables

To determine which single environmental factor has the most influence on tree growth, it was necessary to correlate growth with all available environmental measurements. Available data included temperature, precipitation, and aggregate measures of the environment such as PDSI and PHDI (see Appendix A), and discharge. Initial correlations were made with annual ring indices on monthly environmental data. Correlations were made for the 12 months of the growth year, and September through December of the previous year. Since it is likely that tree growth responds to environmental conditions from a number of months, consecutive months with relatively high correlation values were combined into seasonal variables. Overall, the highest correlations were found between growth and discharge from the Mississippi River, recorded at Thebes, Illinois. Further discussion on relationships between growth and environmental variables follows. Appendix C contains a summary of all correlation results.

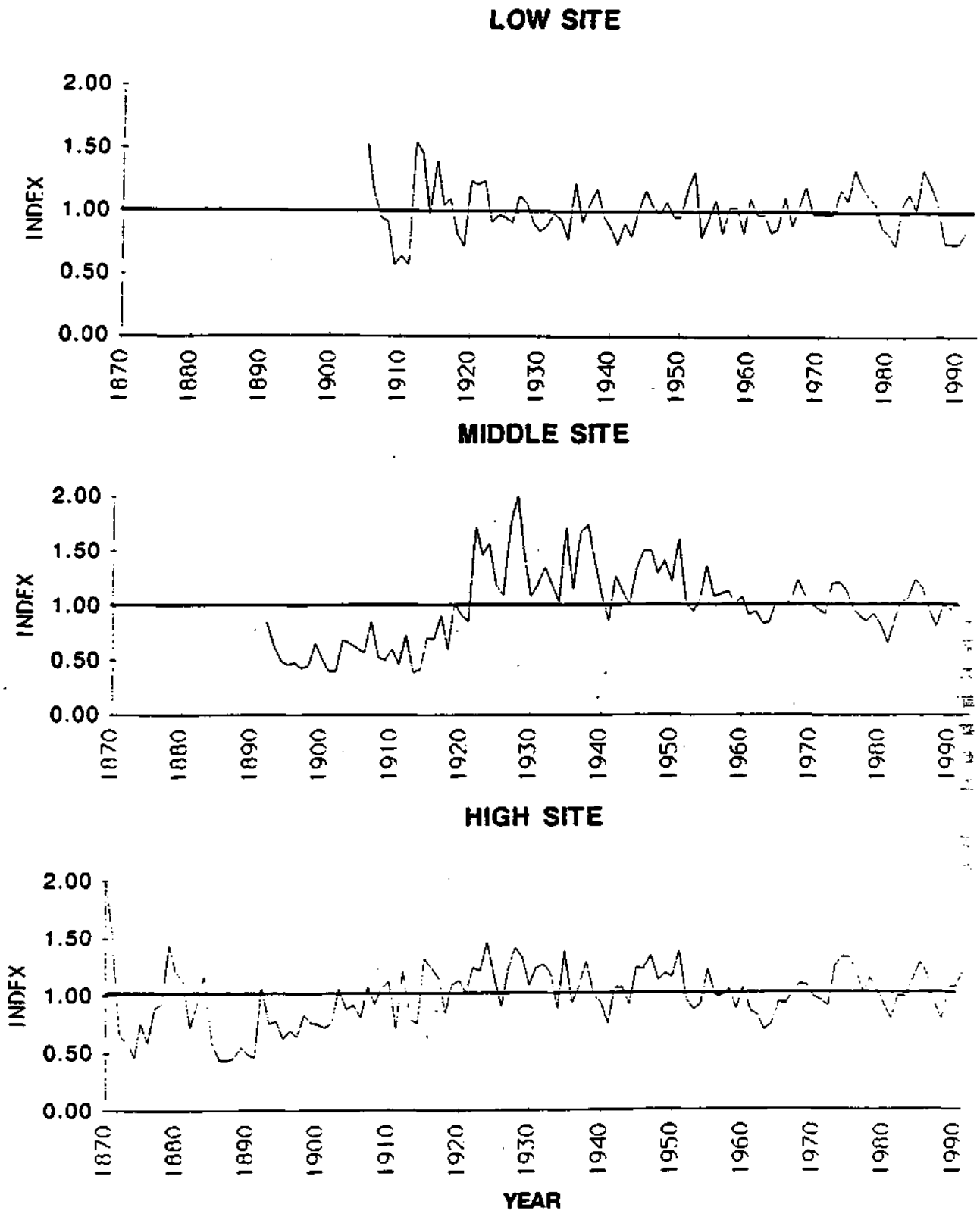

Figure 11. Standardized chronologies for the floodplain, mid-slope, and high level sites at Dillon Bend.

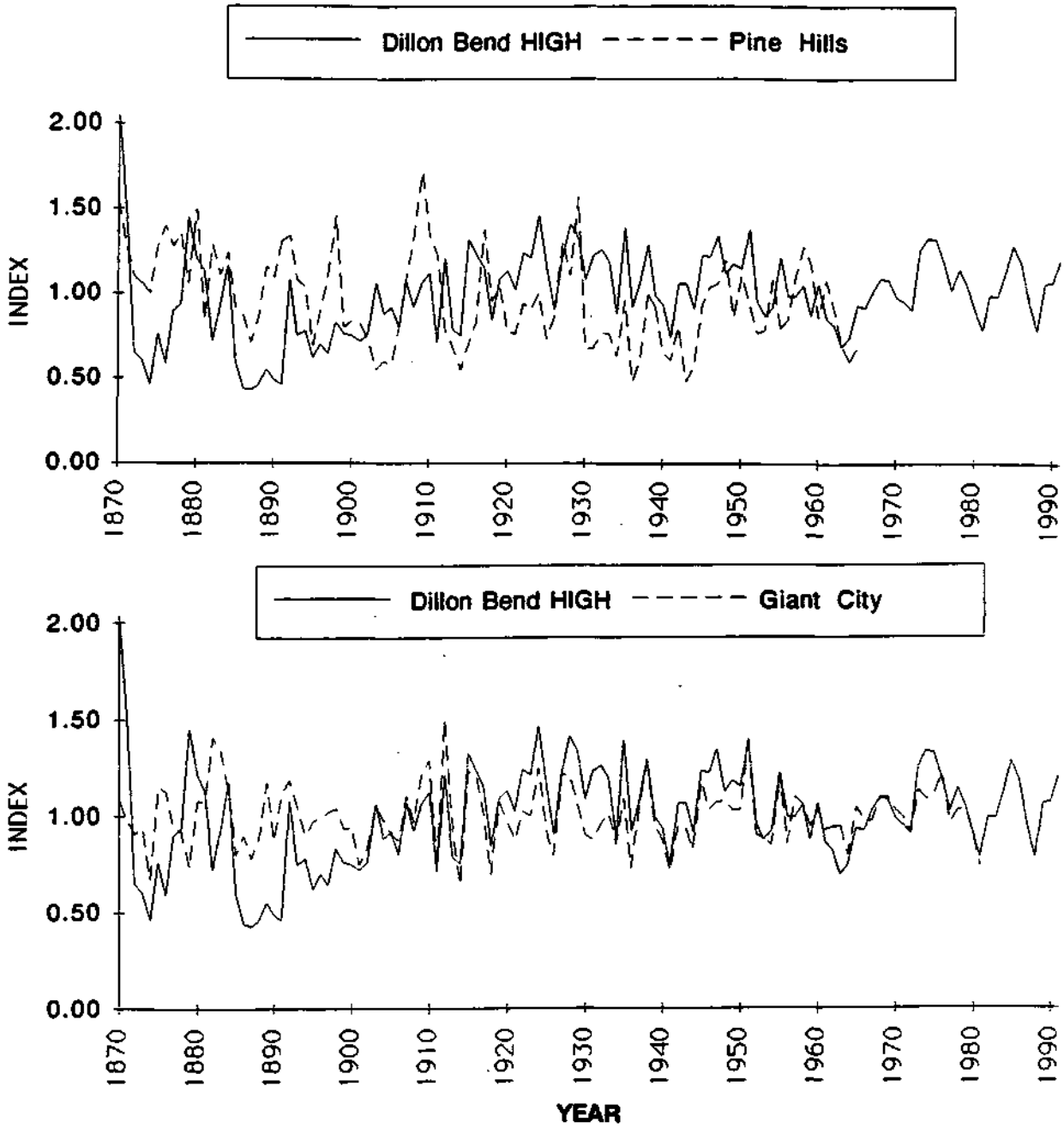

Figure 12. Standardized chronology from the Dillon Bend high site (several species of oak) plotted against TOP: Estes' Pine Hills site (shortleaf pine), and BOTTOM: Duvick's Giant City State Park site.

4.B.1 Correlation with temperature

Pearson correlation coefficients were computed for the floodplain, mid-slope, and high-level chronologies to determine their relationship with (1) regional (Illinois Climate Division 8), (2) Anna, and (3) Carbondale mean monthly maximum temperature. Mean maximum temperature was used since extremely warm weather is a limiting factor to ring growth during the growing season. As expected, computed relationships were significant at the 0.05 level only during the growing season months. With all cases, the high-level upslope trees were most sensitive to maximum temperature. This is probably due to the fact that extremely warm temperatures during the growing season increase evaporation and moisture stress to typically moisture sensitive trees (because of slope drainage). Therefore, ring growth should be, and was negatively correlated with maximum temperature.

The strongest negative temperature correlations in this study were with data from Anna during May through June of the growth year, with coefficients for mid-slope and high trees of -0.31 and -0.51, respectively. Results were not significant for the floodplain chronology.

High temperatures in the latter part of the growing season were less effective since the majority of the annual ring forms early in the season, while growth in July slows considerably (latewood) and usually ends sometime in August. Also, temperatures in the early spring months had a less significant impact on growth. These seasonal characteristics are confirmed by a dramatic decrease in correlation value in the months prior to May and after June (see Appendix tables C.4 through C.6).

Data from Anna provided slightly higher correlations than Carbondale, despite the fact that Carbondale is slightly closer than Anna (20 vs. 25 km). This is most likely due to similarities in topography between Anna and the Dillon Bend area. Regional temperature data did not correlate as well as Anna data. Since temperature tends to be uniformly distributed with latitude, the accuracy of estimates for a specific point is very dependent upon its location within the region. Only in rare cases does a local temperature conform to a regional average.

4.B.2 Correlation with precipitation

The spatial distribution of precipitation is complex, and horizontally discontinuous (Critchfield, 1983). Therefore, it would be expected that the study site, in the long run, would realize some precipitation characteristics with Carbondale, Anna, and the region (Illinois Climate Division 8). This is indeed the case, as there are significant correlations with all three variables. The high level chronology had a 0.51 correlation coefficient with May- August precipitation at Carbondale. The mid-slope chronology best correlated with Anna May-June precipitation at 0.45. The low floodplain trees were much less sensitive, with no single dominant season. Floodplain correlations ranged from 0.30 to 0.35 for relationships to growing season precipitation and also a lagged response to rains from the previous season. Mid-slope and high level trees also exhibited correlation to last growing season's precipitation. The previous August consistently

showed the strongest lagged influence, with correlation coefficients as high as 0.45 for high level trees.

4.B.3 Correlation with PDSI and PHDI

Overall, monthly indices of PDSI and PHDI for Illinois Climate Division 8 had a weaker relationship to tree growth than precipitation, although there were significant correlations at the 0.05 level of confidence for months during and prior to the growing season. Weaker correlations are not surprising since PDSI and PHDI have an appreciable lag time to soil moisture inputs (see Appendix A). The floodplain and mid-slope level trees had weak correlations for all months, as only the most moisture sensitive trees (high level) had correlation coefficients exceeding 0.40. The highest correlations with PDSI occurred in May (0.46) and June (0.47) of the growing season with the high level trees.

There were some relatively strong correlations for high level tree growth and monthly PHDI, but interpretation of the results was difficult. The highest coefficients were found with the current year's September (0.46), October (0.49), and November (0.46). Growth may continue through September, but only rarely continues into early October (Kramer and Kozlowski, 1960). These correlations may be spurious unless growing season droughts for this area naturally continue through the fall months.

4.B.4 Correlation with discharge

Tree-ring growth indices from the floodplain, mid-slope, and high level chronologies were compared to mean monthly discharge data from stream gages at Murphysboro and Thebes, Illinois. Murphysboro is located 10 km upstream from Dillon Bend on the Big Muddy River, and Thebes is 51 km downstream on the Mississippi River. Correlations between growth and Thebes discharge proved to be much stronger than those with Murphysboro, and best overall from the tested environmental variables. Despite the fact that the study site is located on the Big Muddy River, it is not surprising that trees there are affected by flow from the Mississippi. As discussed in section 2.E, the lower section of the Big Muddy is known to backflood with high flows of the Mississippi River.

The highest Thebes correlation (0.57) was with the high level trees for the period of January through July. Also very high was the floodplain correlation (0.53) for the period of previous October through current May, making Thebes discharge the only variable that had a strong relationship with floodplain trees. The correlation coefficient for mid-slope trees was not as impressive (0.40) as results for floodplain and high level trees. As this was the case with correlations with other variables, I suspect that the small sample size of mid-slope trees (9 vs. 12 floodplain and 17 high-level) prevented determination of a clear climatic signal.

The fact that high level trees have such a strong correlation with discharge can be attributed to either or both of two reasons. The first explanation is that these trees are responding only to precipitation, which is the primary water-balance input leading to runoff. Second, despite their above-floodplain location, the root systems of these trees are sensitive to the rising and falling of floodwaters at Dillon Bend. Logic leads to the conclusion that the latter explanation applies. Response to precipitation alone is unlikely, because the discharge at Thebes results from runoff occurring in the entire Upper Mississippi River watershed. The precipitation (and runoff) of the Big Muddy River watershed is not representative of precipitation in the vast area of the Upper Mississippi watershed. In addition, a significant portion of Mississippi River runoff is attributed to spring melting of the northern and alpine snowpack. Physical verification of the depth of Dillon Bend root systems is impossible, but there are indications that they extend deep enough to be affected by the rise and fall of the river. Oak trees have the characteristic of developing a very long taproot, especially on moisture-poor sites (Estes, 1970; Holch, 1931; Kramer and Kozlowski, 1960). The roots of bur oak have been measured at depths of over 2 m after just two growing seasons (Holch, 1931), and roots of more mature trees are known to extend to depths of greater than 10 m (Kramer and Kozlowski, 1960). The high level oak trees are located between 6 and 18 m above the lowest floodplain level, with most trees in the 6-12 m range. During a January 1993 trip to the study site, watermarks were observed on the trees and measured to be 1.1 m above the low floodplain, most likely within reach of at least some of the high level tree's roots. That January 1993 flood was associated with a stage of 9.7 m recorded at Thebes, not a major flood relative to other known high flows. So it is very probable that major backwater floods attained stages at Dillon Bend that provided moisture to the roots of mid-slope and high level trees.

Now that the best correlated environmental variable (discharge at Thebes) has been identified, it is possible to reconstruct past discharge using regression analysis.

4.C Regression analysis results

4.C.1 Model Development

Model development began with data retrieval on dependent and independent variables. Dependent variables were the floodplain and high level tree-ring chronologies. Mid-slope trees were not included in regression analysis because of weaker correlation with discharge and other environmental variables. Independent variables were Thebes October (prior year) through May (growth year) discharge for the floodplain trees, and Thebes January-July (growth year) discharge for the high level trees.

The discharge data set (1934-1991) was divided into 2 equal parts: calibration and verification. Regression analysis was conducted using the Statistical Analysis System (SAS) computer package. The SAS program performs an Analysis of Variance (ANOVA), computes adjusted coefficient of determination ($r^{2)}$, and gives regression parameter estimates. In developing

each regression, output statistics were examined for individual outlier years that might disproportionately influence the form of the fitted regression line.

Outlier identification:

Outliers were identified if any of the following criteria were met (recommended by Laboratory of Tree-Ring Research personnel): Cook's D exceeds 0.10, observed discharge differs more than 2.0 standard deviations from predicted, or Studentized Residual greater than or equal to the absolute value of 2.0.

The Cook's D test measures the changes to the parameter estimates that would result from deleting each observation one at a time, and Studentized Residual is the ratio of the residual (actual minus predicted) over its standard error (Joyner, 1985). According to these criteria, standardized growth indices for 1943, 1968, 1975, and 1977 were identified as outliers in the floodplain regression. Outlier years in the high-level regression were 1955, 1962, 1977 and 1983. Investigation of data for Thebes showed that there was flooding in some of the outlier years: 1943, 1962, 1975, and 1983. The ring width indices for these outlier flood years were relatively narrow compared to other rings in the chronology. Flooding may have inundated the floodplain to the point that tree growth was inhibited for those years. The other outlier years (1955, 1968 and 1977) had relatively low flow all through the growing season, but yet fairly wide growth rings. Carbondale climate data for those years shows that precipitation was near long-term average during the growing season, so trees probably did not experience moisture stress, and realized healthy ring growth.

Parameter estimates:

Each of these outlier years were eliminated from the data, and regression equations were finalized. Regression equations for the two halves of the data set, (1934-1963) and (1964-1991), were evaluated by their values of explained variation, or adjusted r^2. The early period (1934-1963) exhibited slightly higher values of adjusted r^2 for both the floodplain (0.41) and high level (0.45) chronologies, so it was used to calibrate the model. The later period data (1964-1991) was set aside for use in verification of the model. The final regression equations to estimate October-May and January-July Thebes discharge amounts were

$$Q(\text{October-May}) = -24395 + 67352X \qquad (1)$$
$$Q(\text{January-July}) = -17404 + 59664X \qquad (2)$$

where X is the ring width index for a particular year, and Q is total discharge (m^3/s) for the seasonal period. Values of the F-ratio for (1) and (2) are 18.9 and 21.3, respectively. Their acceptance at the 99.9% level of confidence assures that the slope parameters are significantly different from 0.0. It was next necessary to test the accuracy of (1) and (2) as predictors of seasonal discharge.

4.C.2 Verification of regression model

To test the accuracy of the regression equations, each equation was used to predict seasonal Thebes discharge for the 1964-1991 period. Using the computer program VERIFY (Holmes, et al., 1986), the predicted values of discharge were then compared with actual data. The floodplain and high-level regression equations passed all verification criteria, as listed in Table 11.

Using these equations, it was possible to reconstruct seasonal discharge at Thebes through the length of the floodplain or upland tree-ring chronologies. After extending the hydrologic record, patterns and trends of discharge variability at Thebes were examined. To do this, reconstructed and actual Thebes discharge was plotted using both the high and low chronology regression equations. The reconstruction from high level trees provided a more extensive record, dating to 1869, and was the focus of analysis. The analysis began with comparing discharge plots from the gaged period (1934-199l)(Figure 13).

Verification of Floodplain Regression

	VALUE OBTAINED	VALUE OF 95% CONFIDENCE
Correlation	0.48	≥ 0.32 passed
Reduction of error	0.24	≥ 0.10 passed
T-value	1.80	≥ 1.71 passed
Sign-products	6	≤ 9 passed

Verification of High Level Regression

	VALUE OBTAINED	VALUE OF 95% CONFIDENCE
Correlation	0.56	≥ 0.32 passed
Reduction of error	0.39	≥ 0.10 passed
T-value	2.16	≥ 1.71 passed
Sign-products	6	≤ 9 passed

Table 11. Results of verification of the floodplain and high level regression equations, based on comparison of computed test statistics and verification criteria.

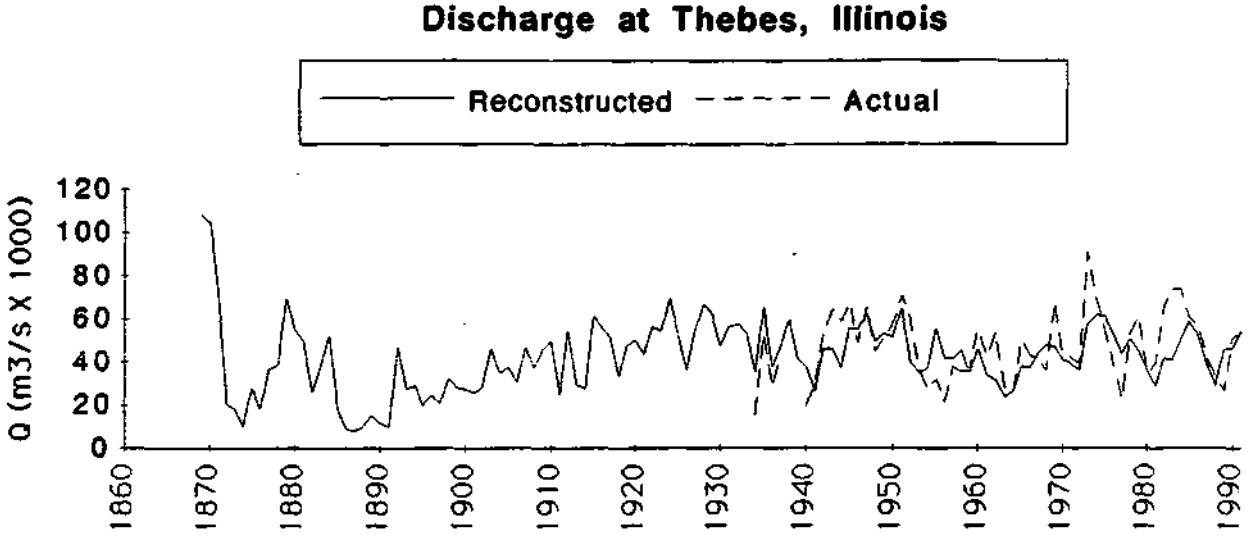

Figure 13. Actual and reconstructed January through July discharge for Thebes, Illinois, from regression based on high-level trees.

Trends in the gaged portion of the plot are in general agreement, but the amplitude of reconstructed discharge is often less than actual extremes of flow. Characteristics of regression analysis provide a plausible explanation. Values of adjusted R^2 for the floodplain and high level regressions were 41% and 45%, respectively. As values of R^2 become small, the variance explained by the regression decreases. This results in a reduction in amplitude in reconstructed data versus actual data.

The reconstructed plot exhibits a lagged response to the regional droughts of 1980-81 and 1988, but responds quickly to the increase in flows during the wet years of 1982-86 (Changnon, 1991). It must be recognized that the extreme fluctuations in the earliest reconstructed decade (1870s) may be less reliable than later years, since only 1 tree contributed to the chronology for that time.

Discharge variability in the 1900s was marked by decadal-scale trends, but overall the range was limited between 20k and 90k m^3/s. The years 1870-1900 contain the highest and lowest reconstructed flows for the entire period. Inclusion of flow amplitude data such as these could have an effect on flood-frequency computations, and possibly call for a re-evaluation of flood control projects. To investigate this possibility, the actual and reconstructed January through July discharge were used to construct flow frequency curves (Figure 14). In general, the reconstructed probabilities slightly underestimate the magnitudes of the actual record. An exception occurs in the region of low probability events. Inclusion of higher reconstructed flows significantly increases the magnitude of rare events over what a linear extension of the actual flow curve would have estimated. From this approach, the actual probability curve may be underestimating the magnitude of rare events such as the 100 year or greater floods.

Another approach locates the high reconstructed flows on an extrapolation of the reconstructed curve. This action would place them as 400 to 600 year events. Although neither approach can be proven, the second method is preferred since probability curves are assumed to maintain a smooth form without abrupt changes (Kite, 1977). With this consideration, implications of including reconstructed flows in flood control project design would be less severe.

A third approach concludes the high reconstructed flows of the late 1800s to have been part of an abnormally high flow period (i.e. 1850-1900). Flow frequency based on data from the abnormally high period may be very different from frequency from the gaged period (1934-present). The best conclusion realizes that there may have been increased variability of prehistoric flows over what has been observed in the gaged period. The abnormally high flow period must be confirmed through further tree ring or other proxy analysis.

Confidence in the discharge reconstruction model can also be gained by confirming pre-historic floods with other data sources. Flood-ring analysis at the Dillon Bend site provides evidence for a number of significant fl

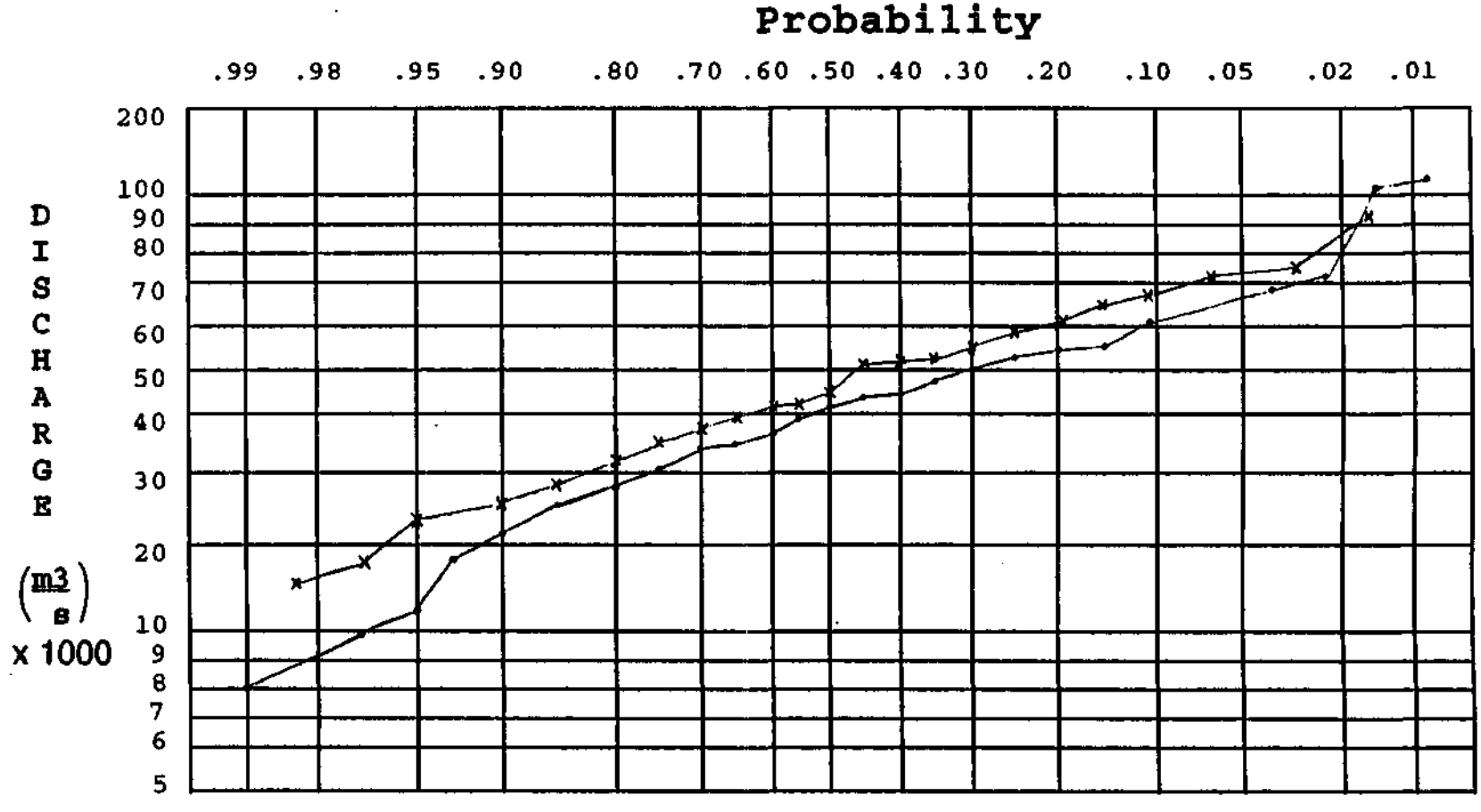

Figure 14. Flow frequency plots constructed of actual (marked by x) and reconstructed (marked by•) January through July discharge for Thebes, Illinois.

4.D Flood ring analysis

All of the floodplain trees (oak and hackberry) and mid-slope trees (oak) were carefully inspected under a microscope for flood rings (see section l.D.l). The entire length of all cores was examined, but rings near the pith and bark were too narrow to conclusively locate flood rings. As a result, no dated flood rings precede the start of stage gage operation (1896). Therefore, the main purpose of the analysis was to determine the effectiveness of the flood-ring reconstruction technique, and its possible application to specific locations on floodplains, such as the Dillon Bend section of the Big Muddy River.

From the examined cores, growth years of discovered flood rings were used to prepare a flood frequency chart (Table 12, Figure 15). There were 83 rings with signs of flooding, all from floodplain trees. Cores reflected the floods of 1947 and 1951 most often, with rings for that year exhibiting a distinct band of enlarged vessels near the end of latewood growth. The intra-ring position of abnormal cells corresponded roughly to timing of the flood within the growing season, considering a growing season that begins in March and ends in August. For example, an flood ring located in the early wood zone may be related to a March or April flood (Table 12). Such interpretations are loose and must be based on growing season length for a particular site.

The 83 flood rings corresponded to 25 individual growth years, each of which corresponded to an annual peak stage of at least 10.3 m documented at Thebes (Table 12); slightly greater than the 9.7 m "rule of thumb" for overbank flooding on the lower Big Muddy River (Ballance, personal communication, 1992). Gaged records reveal that the stage at Thebes equalled or exceeded 9.7 m in 45 years over the stage recorder's period of operation (1896-1991), with 41 of the floods occurring during the growing season (approximately March through September). There are a number of possible reasons why only 61% of the growing season flood years were detected.

First of all, response of trees are likely dependent upon flood magnitude. It is unlikely that flood magnitude was great enough inundate tree crowns, unless the flooding occurred early in the tree's life. So, defoliation flood rings did not exist. The source of flood evidence is left to white flood rings caused by longer-duration, but non-inundating) events. The key factor is a flood duration long enough to cause rapid shoot growth (Yanosky, 1983).

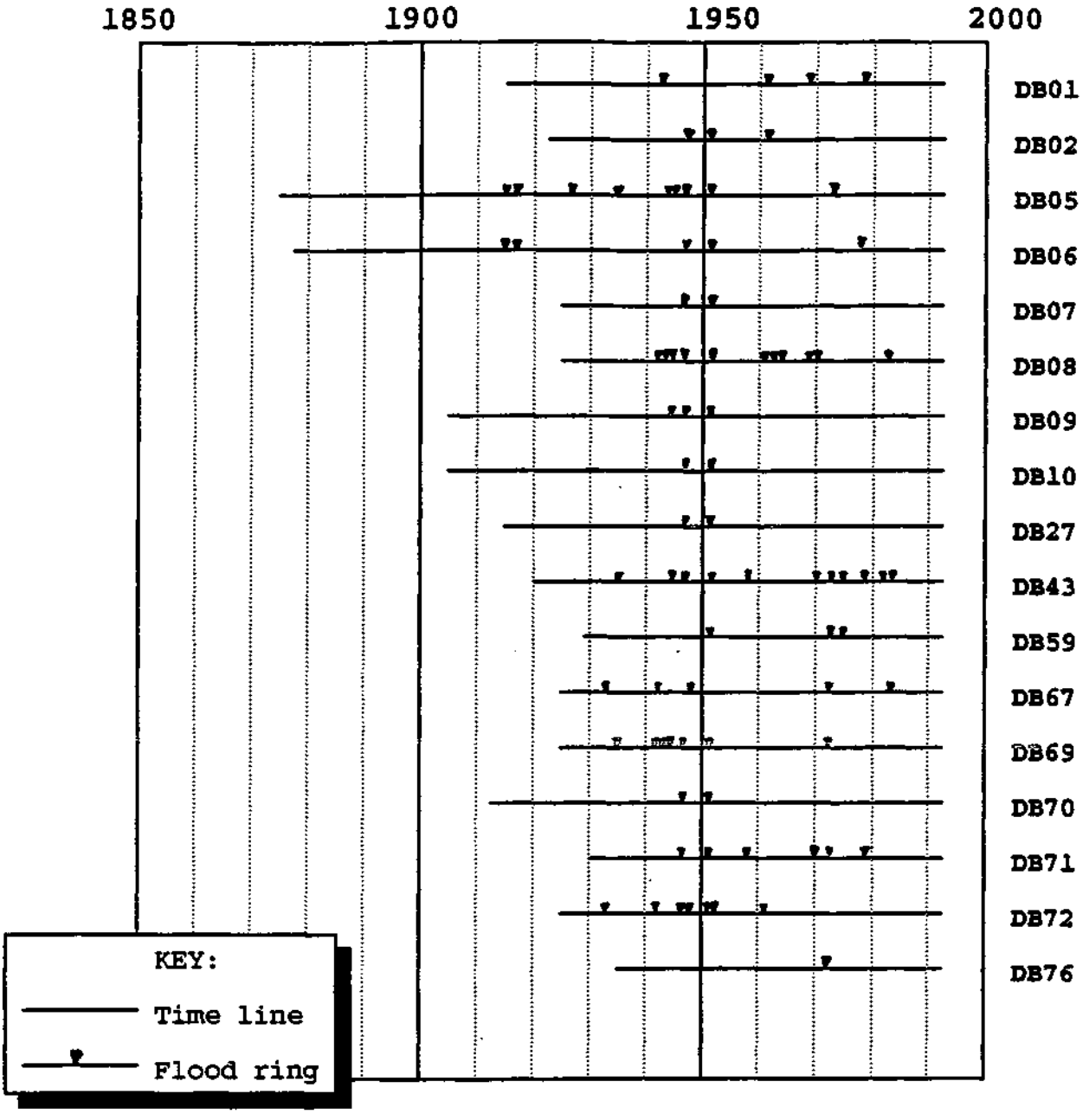

Figure 15. Time scale plot of flood rings discovered after examining floodplain oak and hackberry trees.

year	Flood ring position	Intra-ring cores	Oak cores	Hackberry	Peak stage at Thebes
1915	MLW	2	0		10.4 m, Aug 24
1917	MLW	2	0		10.4 m, Jun 16
1927	ELW	1	0		12.2 m, Apr 20
1933	MLW	1	1		10.4 m, May 19
1935	MLW	4	0		11.1 m, Jun 11
1942	MLW	1	1		10.8 m, Jun 30
1943	MLW	1	0		12.9 m, May 27
1944	ELW	2	1		12.4 m, May 2
1945	EW	5	1		11.8 m, Apr 4
1947	LLW	10	4		12.1 m, Jul 6
1948	EW	0	2		11.2 m, Mar 28
1951	LLW	9	5		12.1 m, Jul 24
1952	ELW	1	1		11.4 m, May 2
1958	LLW	1	1		10.3 m, Jul 25
1960	ELW	1	0		11.3 m, Apr 11
1961	ELW	3	1		11.8 m, May 13
1962	ELW	1	0		11.0 m, Mar 27
1969	MLW	2	0		11.8 m, Jul 15
1970	MLW	2	1		11.0 m, May 5
1973	EW	2	4		13.2 m, Apr 30
1978	EW	1	0		11.6 m, Mar 29
1979	EW	2	1		13.1 m, Apr 17
1983	ELW	2	1		12.1 m, May 6
1984	ELW	1	1		11.7 m, Apr 27
1985	EW	1	0		12.3 m, Mar 1

Table 12. Information on flood rings from floodplain trees at Dillon Bend. Included are: year, intra-ring position, number of verifying cores, and stage and date of related flooding at Thebes. Codes for intra-ring position are: EW (earlywood), ELW (early-latewood), MLW (mid-latewood), LLW (late-latewood)

The final phase of flood ring analysis was stage investigation. Since the floodplain at Dillon Bend has about 1 m of relief relative to the river surface, a small magnitude event would most likely produce flood rings only in the lowest trees. A higher magnitude event may produce flood rings in both elevated and low trees. The core which held the most flood rings was from the lowest-lying tree (hackberry). The lowest trees had the benefit of maximized duration, being affected through the rising and falling of the floodcrest while higher trees may be flooded only briefly. Comparison between tree elevation and magnitude data did not reveal any clear stage influence, probably because the duration of floodwaters at some threshold level is most important for flood ring formation. It was interesting to note, however, that there was a distinct level above which trees no longer contained flood rings. This began at a point 2.7 m above the lowest level of the floodplain. It can be concluded that floods of damaging duration have not risen above that stage over the period of the tree-ring chronology at this site.

Flood ring information provides a means of relating gaged stage data to resulting water level at other locations, or reconstructing flood history for a river lacking hydrologic data. There are obvious benefits from this work for agriculture and construction, for those industries are highly dependent on flood stages in fields or developed areas, not on the actual discharge at some distant gaging station. The flood ring analysis technique is especially useful on rivers, such as the Big Muddy, that are influenced by flow from another drainage basin.

4.E Results of elevational comparisons

The initial step in an elevational analysis of ring widths was computation of correlation coefficients between floodplain/high-level index ratios (dependent variable) and hydrologic data from Thebes, Illinois. Peak annual stage was chosen as the independent variable, since the maximum height of floodwaters determines degree of tree inundation more than a seasonal aggregate of discharge. Results in the linear correlation analysis were not significant at the 95% level of confidence, and it was evident that an alternate approach to the problem was necessary.

When considering the floodplain/high-level ratio concept, it is important to recognize the possibility of thresholds. That is to say, there may be a threshold of peak stage above which floodwaters will cause inhibited ring growth in floodplain trees. Also there may be a threshold of the ratio itself; a significant departure from 1.0 which corresponds to abnormal comparative growth from flooding. The threshold concept can be investigated through the use of categorical variables and Analysis of Variance (ANOVA), which will conclude whether or not there are explained differences between the categories. The ANOVA approach, and its underlying assumptions will be explained in detail in the remainder of this section.

4.E.1 Assumptions of ANOVA

The One-Way ANOVA test is concerned with differences between classes, and uses the class means, sums of squares, and estimates of variance to summarize their characteristics (Clark

and Hosking, 1986). Total variance in the data is divided into explained (between class) and unexplained parts (within class). A ratio (F) of between/within class variance is determined. If between-class variance is significantly greater than within-class variance, the null hypothesis of "no difference between categories" will be rejected. A level of confidence of 95% was chosen as a reasonable interval estimate for parameters.

4.E.2 Variables

The two variables used in the ANOVA were *ratio,* and *stage.* The main principle behind using the floodplain/high-level ratio is that values of ratio near 1.0 indicate similar growing conditions between the two sites. Positive departures from 1.0 indicate enhanced floodplain growth from flood-delivered moisture, while negative departures show inhibited floodplain growth from inundation.

The degree of departure required for each of these effects was estimated by adding and subtracting the value of 0.10, which is 10% of the equal-site growth ratio, to the equal-site growth ratio (1.0). The resulting threshold for flood enhanced growth was: *ratio* > 1.10, and for flood-inhibited growth: *ratio* < 0.90. When *ratio* meets either of these criteria, flooding is determined to have occurred in that year. Threshold for the peak *stage* variable was set at 9.7 m, since the river is known to overflow the banks when the Thebes stage reaches that level (Ballance, personal communication, 1992). All years with stages greater than 9.7 m were labeled flood years.

Each year of the chronology was listed with its corresponding value of ratio and stage. The variables were then assigned categorical variables of either 1 (flooding) or 0 (no flooding) according to the criteria previously described (see Table 13). When categorical values agree for a year (both 0 or 1), the ratio measure accurately recorded the presence or absence of a flood. With the thresholds determined for Dillon Bend, the variables agreed 66% of the time, and 70% Thebes floods at or above 9.7 m were detected.

Most of the errors (13 of 19) occurred when an actual flood was not reflected by the ratio variable. The probable cause is that those missed floods were not of sufficient duration to alter ring growth. There were 4 cases of small ratio values with no flooding. It is possible that dry conditions did not affect trees on the slope as much as those on the floodplain, since slope trees are more adapted to stressful environmental conditions. In only 2 cases when the ratio was > 1.10 did flooding not occur.

Year	Ratio	/ Cat.	Stage	/ Cat.	Agree?	Year	Ratio	/ Cat.	Stage	/ Cat.	Agree?
1934	0.88	1	6.2	0	No	1970	1.00	0	11.0	1	No
1935	0.88	1	11.0	1	Yes	1971	1.02	0	10.0	1	No
1936	0.99	0	7.7	0	Yes	1972	1.10	1	10.0	1	Yes
1937	0.98	0	9.2	0	Yes	1973	0.94	0	13.2	1	No
1938	0.91	0	9.5	0	Yes	1974	0.81	1	11.0	1	Yes
1939	0.96	0	11.0	0	No	1975	1.01	0	11.0	1	No
1940	0.92	0	6.0	0	Yes	1976	1.01	0	9.2	0	Yes
1941	0.99	0	8.9	0	Yes	1977	1.09	0	7.8	0	Yes
1942	0.85	1	10.8	1	Yes	1978	0.94	0	11.6	1	No
1943	0.75	1	12.2	1	Yes	1979	0.84	1	13.1	1	Yes
1944	1.10	1	11.9	1	Yes	1980	0.90	1	9.5	0	No
1945	0.94	0	11.5	1	No	1981	0.92	0	9.0	0	Yes
1946	0.84	1	10.2	1	Yes	1982	1.05	0	9.0	0	Yes
1947	0.72	1	12.2	1	Yes	1983	1.16	1	11.0	1	Yes
1948	0.96	0	10.2	1	No	1984	0.89	1	11.7	1	Yes
1949	0.81	1	9.5	0	No	1985	1.04	0	12.3*	1	Maybe
1950	0.83	1	9.8	1	Yes	1986	1.03	0	12.1*	1	Maybe
1951	0.86	1	12.1	1	Yes	1987	1.14	1	12.6	1	Yes
1952	1.38	1	11.4	1	Yes	1988	0.96	0	9.5	0	Yes
1953	0.91	0	8.1	0	Yes	1989	0.70	1	11.0	1	Yes
1954	1.01	0	6.8	0	Yes	1990	0.69	1	12.1	1	Yes
1955	0.89	1	7.4	0	No	1991	0.69	1	9.7	1	Yes
1956	0.83	1	5.6	0	No						
1957	1.04	0	9.7	0	Yes	Number of years in agreement: 39 of 56, or 66%					
1958	0.98	0	10.3	1	No						
1959	0.94	0	7.9	0	Yes	*Non-growing season floods (not included in study).					
1960	1.04	0	11.3	1	No						
1961	1.13	1	11.8	1	Yes						
1962	1.18	1	11.0	1	Yes						
1963	1.20	1	8.3	0	No						
1964	1.16	1	7.5	0	No						
1965	1.19	1	10.4	1	Yes						
1966	0.96	0	9.9	0	No						
1967	1.02	0	10.3	1	No						
1968	1.09	0	8.6	0	Yes						
1969	0.90	1	11.8	1	Yes						

Table 13. Values of categorical variables ratio and stage, and prediction agreement statistics for each year of the combined floodplain/high-level chronology.

4.E.3 Results of ANOVA

ANOVA was run on the categorical variables ratio and stage, to determine if there is a difference between the non-flooding ratio (0.90 < *ratio* < 1.10) and the flooding ratio (0.90 > *ratio* > 1.10). The null hypothesis, Ho, is that there is no difference between the populations for the two *ratio* classes. ANOVA results are shown in Table 14. The rejection region at the 95% level of confidence is F > 4.0. Since the calculated F is 5.76, the null hypothesis is rejected and it is concluded that there is a significant difference between the two ratio categories.

The preliminary results of the comparative technique are promising, especially since it detected Dillon Bend floods slightly better than the flood ring technique (66% vs. 61%). Both approaches have potential for improved success, and should be tested at other locations.

Analysis of Variance

Source of variation	SS	df	MS	F	Prob > F
Between groups	1.33	1	1.34	5.76	0.02
Within groups	13.01	56	0.23		
Total	14.34	57			

Table 14. Results of Analysis of Variance between categorical measures of the floodplain/high-level ratio variable, and a categorical measure of peak annual stage. (SS=sum of squares; MS=mean sum of squares;, df=degrees of freedom; $F=MS_{between}/MS_{within}$).

CHAPTER 5
SUMMARY AND CONCLUSIONS

It is possible to reconstruct flood events on the Big Muddy River using any of 3 methods: 1) regression of ring width with gaged discharge; 2) flood ring analysis; and 3) floodplain/upland tree comparison. The regression approach models Thebes seasonal (i.e. January through July) discharge as a function of standardized ring-width indices of upslope trees. Flood ring analysis associates abnormalities in the wood tissue of a growth ring to physiological impacts of flooding. Comparison of floodplain and upland trees relies on the premise that floodplain trees have inhibited ring growth when a flood event results in prolonged soil saturation, while upland trees have enhanced or normal growth. Each of these approaches in dendrohydrology contains unique information on past flooding and holds special potential application for Illinois and other midwestern states, since much of the region's development is located along waterways within the Mississippi River basin.

Regression of ring width on discharge gives an indication of the overall hydrology (i.e. low flow, high flow) of the years which comprise the tree-ring chronology. A time line of aggregate discharge is constructed, from which patterns, trends, and extremes can be extracted. Flood ring analysis and floodplain/upland tree comparisons are mainly used to determine a prehistoric flood chronology for the study site. Rings which are determined to reflect flooding are assigned calendar years which can be used to construct a flood-frequency plot for the site. Flood ring analysis can also provide some flood magnitude information, by noting the elevation at which trees no longer exhibit flood rings. When the 3 described approaches to flood reconstruction are applied simultaneously, many characteristics of flooding for a particular site are revealed.

The study site, located along the Dillon Bend section of the Big Muddy River, was cored extensively for flood reconstruction. A total of 62 cores were collected from 23 oak trees and 8 hackberry trees. The study area was divided into 3 separate collection sites: floodplain, mid-slope and high-level trees. Standardized ring-width indices from the floodplain and high-level trees were regressed on seasonal aggregates of Thebes discharge, in order to compute a discharge reconstruction model. The resulting equations, when used with the ring-width data, extend seasonal Thebes discharge information (January through July) from 1934 to 1870. The extended discharge data shows that the years 1870 to 1900 contained the highest and lowest flow seasons for the entire period (1870 to 1991). Inclusion of reconstructed discharge into flood frequency calculations reveals that studies based on gaged data may be underestimating the magnitude of rare flood events at Thebes.

Inspection of floodplain cores for flood rings lead to the discovery of 83 such abnormal rings. Comparison of tabulated flood ring results to Thebes stage data, showed that the technique detected 61% of floods above 9.7 m. There was a distinct level on the landscape above which trees no longer contained flood rings, giving a rough estimate of a local peak stage for the length of the chronology (87 years).

The elevational comparison technique was more successful in detecting flood events than the flood ring technique (70% vs. 61%). A ratio of floodplain/high-level standardized ring-width indices was calculated and compared to peak annual stage data for Thebes. The ratio and stage data were converted into categorical variables for analysis of variance (ANOVA). It was determined that there is a difference between flooding and non-flooding ratio variables, which detected 70% of the Thebes floods above 9.7 m.

Considering that flooding is one of the most damaging and costly weather-related disasters in the United States, the importance of successful floodplain management cannot be disputed. Since funding for management is limited, it is necessary to design measured and practical flood control systems. Current methodology uses stream gage data to estimate the magnitude and frequency of floods for a particular river. When this method is based on a short period of record, which is the case for much of Illinois and the United States, evaluation of the magnitude of rare flood events becomes difficult. This problem can be alleviated with the inclusion of proxy flood data from other sources. Tree-ring analysis has proved to be a valuable source of paleoflood data. Inclusion of reconstructed discharge in flood frequency estimates could prompt a reassessment of existing flood control projects, and influence the design of future protection. Dendrohydrology also has the flexibility of giving past-flood information at a particular site, which may be far removed from a gaging station. The economic advantage to developers, farmers, and current residents are obvious, in addition to the potential savings of lives and property.

With this in mind, dendrohydrology should continue to be tested on other rivers, with other tree species, and new techniques should be investigated.

ACKNOWLEDGEMENTS

I would like to thank my advisor, Wayne M. Wendland, for direction in conducting this research, and for many hours of field assistance and patient manuscript review. Thanks also to Henri Grissino-Mayer, who aided in the computational aspects of dendrochronology, and to others from the Tree-Ring Laboratory in Arizona who gave me advice and training in dendrochronology. Also, this work would not have been possible without support form the Midwest Climate Center.

I appreciate the help of committee members Scott Isard and Richard Phipps. I am grateful to Donald Johnson for geomorphic consulting and work at the study site. Thanks, too, to field workers Dean Olson, Paul Jahn, and Dave Grimley.

The following people and/or agencies were very helpful in providing information and other types of assistance: Beth Shimp, U.S. Forest Service (Harrisburg Office); Dr. Lawrence R. Stritch, Zone Botanist Shawnee/Wayne-Hoosier National Forests; Gary Balding, U.S. Geological Survey, Water Resources Division (Urbana office); Illinois State Water Survey, Surface Water Section; Illinois State Water Survey, Climate Section.

Finally, thanks to the U.S. Air Force for allowing me the time and opportunity to complete this program.

References

Ballance, D. 1992: Personal communication.

Biasing, T.J., and **D.N. Duvick** 1984: Reconstruction of precipitation history in North American corn belt using tree rings. *Nature,* 307: 143-145.

Changnon, S.A.. 1991: *Global Climate Change and Illinois.* Illinois State Water Survey miscellaneous publication 131.

Gark, W.A, and P.L. Hosking. 1986: *Statistical Methods for Geographers.* New York: Wiley & Sons.

Critchfield, H.J. 1983: *General Climatology.* New Jersey: Prentice-Hall.

Dobney, F.J. 1975: *River Engineers on the Middle Mississippi.* Washington, D.C.: U.S. Government Printing Office.

Estes, E.T. 1970: Dendrochronology of black oak (Quercus velutina Lam.), white oak (Quercus alba L.), and shortleaf pine (Pinus echinata Mill.) in the central Mississippi valley. *Ecological Monographs,* 40: 295-316.

Fieldhouse, D.J., and **W.C. Palmer.** 1965: Meteorological and agricultural drought. *University of Delaware Agricultural Experiment Station, Bulletin 353.* 1-71.

Fritts, H.C. 1965: Tree ring evidence for climatic changes in western North America. *Monthly Weather Review,* 93: 421-443.

Fritts, H.C. 1965b: The relation of growth rings in American beech and white oak to variations in climate. *Tree-ring Bulletin,* 25: 2-10.

Fritts, H.C. 1976: *Tree-Rings and Climate.* London: Academic Press.

Fritts, H.C. 1991: *Reconstructing Large-scale Climatic Patterns from Tree-Ring Data* University of Arizona Press: Tucson.

Gill, C.A 1970: The flooding tolerance of woody species; A review. *Forestry Abstracts,* 31: 671-687.

Gottesfeld, A.S., and L.M. Johnson-Gottesfeld. 1990: Floodplain dynamics of a wandering river, dendrochronology of the Morice River, British Columbia, Canada. *Geomorphology,* 3: 159-179.

Grissino-Mayer, H.D. 1992: Personal communication.

Harris, S.E., Jr., C.W. Horrell, and **D. Irwin.** 1977: *Exploring the Land and Rocks of Southern Illinois.* Illinois: SIU Press.

Herman, R.J. 1979: *Soil Survey of Jackson County.* Illinois Agricultural Experiment Station soil report 106.

Hirschboeck, K.K. 1987: Catastrophic flooding and atmospheric circulation anomalies. *in* L. Mayer and D. Nash, Catastrophic Flooding. Boston: Allen and Unwin; pp.23-56.

Holch, A.E. 1931: Development of roots and shoots of certain deciduous tree seedlings in different forest sites. *Ecology,* 12: 259-298.

Holmes, R.L., R.K. Adams, and **H.C. Fritts.** 1986: *Tree-Ring Chronologies of Western North America: California, Eastern Oregon and Northern Great Basin* (with procedures used in the chronology development work including users manuals for computer programs COFECHA and ARSTAN). Tucson: University of Arizona Press.

Hosner, J.F., and **S.G. Boyce.** 1962: Tolerance to water saturated soil of various bottomland hardwoods. *Forest Science,* 8: 180-186.

Hughes, M.K., and **P.M. Brown.** 1992: Drought frequency in central California since 101B.C. recorded in giant sequoia tree rings. *Climate Dynamics,* 6: 161-167.

Illinois Environmental Protection Agency. 1988: *An Intensive Survey of the Big Muddy Main Stem from Rend Lake to the Mississippi River.* IEPA/WPC/91-56.

Isard, S.A., and **W.E. Easterling.** 1989: Predicting large-area corn yield with a weighted Palmer Z-index. *Journal of Climate, 2:* 248-252.

Johnson, D.L. 1992: Personal communication.

Joyner, S.P. 1985: *SAS/STAT Guide for Personal Computers.* California: Brooks-Cole Publications.

Kite, G.W. 1977: *Frequency and Risk Analyses in Hydrology.* California: Brooks-Cole Publications.

Knighton, D. 1984: *Fluvial Forms and Processes.* Edward Arnold: London.

Kochel, R.C., and **Baker, V.R.** 1982: Paleoflood hydrology. *Science,* 215: 353-361.

Kramer, P.J., and **Kozlowski, T.T..** 1960: *Physiology of Trees.* New York: McGraw-Hill.

Kutzbach, J.E., and **Guetter, P.J.** 1980: On the design ofpaleoenvironmental data networks for estimating large-scale patterns of climate. *Quaternary Research,* 14: 169-187.

LaMarche, V.C., Jr. 1974: Paleoclimatic inferences from long tree-ring records. *Science,* 183: 1043-1048.

Martens, D.M. 1992: Dendrochronological flood-frequency analysis: an Australian application. *Australian Geographical Studies,* 30: 70-86.

Martin, C.W. 1992: Late holocene alluvial chronology and climate change in the central great plains. *Quaternary Research* 37, 315-322.

McAlpine, R.G. 1961: Yellow poplar seedlings intolerance to flooding. *Journal of Forestry,* 59: 566-568.

McCord, V.A. 1990: *Augmenting Flood Frequency Estimates using Flood-Scarred Trees.* M.S. thesis, University of Arizona, Tucson, 182 pp.

Michaelsen, J., Hasten, L., and **Davis, F.W.** 1987: 400 years of central California precipitation variability reconstructed from tree-rings. *Water Resources Bulletin,* 23: 809-818.

Mitsch W.J., and W.G. Rust 1984: Tree growth responses to flooding in a bottomland forest in northeastern Illinois. *Forest Science,* 30: 499-510.

Phipps, R.L. 1993: Personal communication.

Phipps, R.L. 1972: Tree rings, stream runoff, and precipitation in central New York - a revaluation. *U.S. Geological Survey Professional Paper* 800-B, 259-264.

Sigafoos, R.S. 1964: Botanical evidence of floods and floodplain deposition. *U.S. Geological Survey Professional Paper* 485-A, 35 pp.

Smith, L.P., and **Stockton, C.W.** 1981: Reconstructed stream flow for the Salt and Verde rivers from tree-ring data. *Water Resources Bulletin,* 17: 939-947.

Stockton, C.W. 1975: *Long-Term Stream flow Records Reconstructed from Tree Rings.* Laboratory of Tree-Ring Research, Paper no. 5. Tucson: University of Arizona Press.

Stokes, M.A. and **T.L. Smiley.** 1968: *An Introduction to Tree-Ring Dating.* Chicago: University of Chicago Press.

United States Army Corps of Engineers. 1945: *Highest and Lowest Annual Stages: Mississippi River and its Tributaries to 1945.* Vicksburg: Mississippi River Commission.

United States Army Corps of Engineers. 1968: *Big Muddy River Comprehensive Basin Study.* St. Louis: Corps of Engineers.

United States Army Engineer District 1970: *Upper Mississippi River Comprehensive Basin Study.* Chicago: Corps of Engineers.

United States Geological Survey. 1990: 7.5 Minute series (topographic) gorham quadrangle. U.S. Government Printing Office.

United States Geological Survey. 1991: Water resources data for Illinois, water year 1991. *U.S. Geological Survey Water-Data Report IL-91-1.*

United States Geological Survey. 1993: Hydrologic data for Murphysboro and Thebes, Illinois. Provided by USGS Water Resources Division, Urbana, Illinois.

Wendland, W.M., and **D. Watson-Stegner.** 1983: A technique to reconstruct river discharge history from tree-rings. *Water Resources Bulletin,* 19: 175-181.

Yanosky, T.M. 1983: Evidence of floods on the Potomac River from anatomical abnormalities in the wood of floodplain trees. *U.S. Geological Survey Professional Paper* 1296, 42 pp.

APPENDIX A: PDSI AND PHDI

Palmer Drought Severity Index (PDSI):

PDSI is a method whereby the agricultural effects of a meteorological drought can be calculated from temperature and precipitation. In its calculation, drought severity is viewed as a function of moisture demand and moisture supply (see Fieldhouse and Palmer, 1965). Therefore, it determines whether or not the water needs of crops (or trees) at a particular location are being met. Since it takes time for serious drought to develop, PDSI takes into account previous and current weather conditions. The developed procedure treats drought severity as a function of accumulated differences between actual and required precipitation, where the requirement depends on rainfall carryovers, evapo-transpiration, moisture recharge, and runoff (Fieldhouse and Palmer, 1965). The computed monthly drought severity index (X) range from about -5.0 to +5.0, and is interpreted by its class of wet and dry periods (Table A.l).

Monthly value of X	Class
≥ 4.00	extremely wet
3.00 to 3.99	very wet
2.00 to 2.99	moderately wet
1.00 to 1.99	slightly wet
0.50 to 0.99	incipient wet spell
0.49 to -0.49	near normal
-0.50 to -0.99	incipient drought
-1.00 to -1.99	mild drought
-2.00 to -2.99	moderate drought
-3.00 to -3.99	severe drought
≤ -4.00	extreme drought

Table A.l PDSI classes for wet and dry periods.

Palmer Hydrologic Drought Index (PHDI):

The "moisture anomaly index" (PHDI, or Z-index) is sensitive to short-term changes in soil moisture, and responds more quickly than PDSI. Therefore, PHDI is a better indicator of agricultural drought than PDSI, since crop growth is highly dependent upon current moisture levels during the growing season (Isard and Easterling, 1989). Tree growth is most sensitive to surface moisture supply, but because of extensive root systems, can also be affected by a lowering of the water table. As a result, tree growth may reflect long term changes in the water table as measured by PDSI.

APPENDIX B: COMPUTER PROGRAMS

Computer programs used in this research were obtained from the Laboratory of Tree-Ring Research, University of Arizona, Tucson. They were developed by Richard Holmes and Edward Cook for the International Tree-Ring Data Bank (ITRDB). A short description of each program follows:

COFECHA:

The main function of COFECHA is identification of dating errors in tree-ring measurements (Holmes, 1983). The dated and measured ring series are filtered by fitting a 20-year cubic spline, and then dividing the series values by the corresponding spline curve values to remove low-frequency variance. The high frequency residual is subjected to a log transformation to equalize proportionally the variability among small and large rings (Holmes, et al., 1986). The mean values of the combined series comprise the master dating chronology. After an initial COFECHA run using all of the ring series, the 10 series with the best correlation to the master are selected to compose a more reliable master dating chronology. Each COFECHA output identifies measuring or counting errors by flagging 40 year ring segments and individual outliers within each core that do not agree with the master. After using the output to account for possible problems in master cores, each of the remaining cores can be added one by one to the COFECHA program and checked against the master chronology. As measuring or counting errors are remedied, each core is included in the final dating chronology.

ARSTAN:

The program ARSTAN produces annual standardized, dimensionless indices for all rings of one core. The first step is to fit either negative exponential curves or stiff cubic splines to tree-ring series (Holmes, et al., 1986). Trend curves differ in form depending upon site-specific growth variations and distance from the pith of the tree. Visual inspection of raw ring-widths is used to estimate whether the trend of growth is a clear departure from negative exponential. ARSTAN prompts as to whether the operator believes there are any cores with clear departures. Specified cores are fitted with cubic splines to model growth trend. An annual index is computed by dividing the measured ring width by the value of the growth curve for that particular year. To account for the lag influence of previous years' growth, ARSTAN uses autoregressive modeling to enhance the common signal (Holmes, et al., 1986). The chronology of a tree core is then expressed as a series of indices that are stationary in both mean and variance (Stockton, 1975).

Master chronologies are constructed by combining the indices from individual cores, and computing an average growth index for each year in the combined chronology.

VERIFY:

The purpose of the VERIFY program is to test the accuracy of the discharge reconstruction model. This is accomplished by comparing predicted values of discharge to actual data that were not included in the determination of the regression parameters. The following test statistics are computed for the data sets at the 95% level of confidence: correlation coefficient, reduction of error, T-value, and sign-products. If any of the computed statistics fail to meet acceptance criteria, the discharge reconstruction model fails.

MEASURE:

The MEASURE software tests the accuracy of ring measurement by comparing original measurements with remeasured ones for the same core. The program prompts the user for the ring-width series for the original and remeasured cores. Descriptive statistics (mean, standard deviation, sensitivity, etc.) are computed for each data set. A difference of means test is conducted at the 95% and 99% level of confidence, and printed results show whether or not these standards are met.

APPENDIX C

Complete results of correlation analysis

Results of linear correlation analysis between floodplain, mid-slope, and high-level growth indices and environmental variables are presented in tabular format (Tables C.l through C.10). Presentation of all correlation results are important to show that tree rings do/do not respond to seasonal environmental variables in explainable degree and fashion. Each table corresponds to a different environmental variable:

Table	Environmental variable
C.l	Illinois regional precipitation
C.2	Anna precipitation
C.3	Carbondale precipitation
C.4	Illinois regional temperature
C.5	Anna temperature
C.6	Carbondale temperature
C.7	Illinois regional PDSI
C.8	Illinois regional PHDI
C.9	Murphysboro discharge
C.10	Thebes discharge

Each row of data are results for one chronology: LOW (floodplain), MID (mid-slope), and HI (high-level). Listed in each row are linear correlation coefficients (r), along with the probability of the null hypothesis (true population correlation coefficient = 0.0), below the correlation coefficient. A 95% level of confidence corresponds to a probability < 0.05.

Months analyzed are October through December after the past growth season, and January through September of the current growth year. The lower half of the table contains correlation results of seasonal groupings of months.

Illinois regional precipitation

Pearson Correlation Coefficients / Prob > |R| under Ho: Rho=0 / Number of Observations

	LMAYP	LJUNP	LJULP	LAUGP	LSEPP	LOCTP	LNOVP	LDECP	JANP	FEBP
LOW	-0.14093	-0.02896	-0.22855	0.28857	0.26500	0.10440	-0.08586	0.14514	0.09153	0.08658
	0.2010	0.7937	0.0365	0.0078	0.0148	0.3446	0.4374	0.1877	0.4077	0.4336
	84	84	84	84	84	84	84	84	84	84
HID	-0.02654	0.12241	-0.24272	0.16268	0.26272	0.22868	-0.03536	0.11258	0.05905	0.00878
	0.8006	0.2424	0.0191	0.1192	0.0110	0.0275	0.7365	0.2826	0.571B	0.9331
	93	93	93	93	93	93	93	93	94	94
HI	-0.03419	0.06400	-0.30638	0.38577	0.24010	0.22389	0.00334	0.21940	0.12285	0.03897
	0.7449	0.5422	0.0028	0.0001	0.0204	0.0310	0.9746	0.0346	0.2381	0.7092
	93	93	93	93	93	93	93	93	94	94

	MARP	APRP	MAYP	JUMP	JULP	AUGP	SEPP	OCTP	NOVP	DECP
LOU	0.39288	0.03472	-0.00021	0.19048	0.04590	0.17100	0.07035	0.02954	0.12899	0.11051
	0.0002	0.7539	0.9985	0.0827	0.6784	0.1199	0.5248	0.7897	0.2422	0.3170
	84	84	84	84	84	84	84	84	84	84
MID	0.01722	0.19144	0.10397	0.35706	-0.06673	0.08333	0.03252	0.19702	0.04894	0.01884
	0.8692	0.0646	0.3186	0.0004	0.5228	0.4246	0.7557	0.0570	0.6395	0.8570
	94	94	94	94	94	94	94	94	94	94
HI	0.04576	0.13721	0.23587	0.36216	-0.02698	0.26837	0.09887	0.23221	0.O8091	0.04926
	0.6614	0.1873	0.0221	0.0003	0.7963	0.0089	0.3431	0.0243	0.4382	0.6373
	94	94	94	94	94	94	94	94	94	94

3 'WITH' Variables: LOU MID HI
9 'VAR' Variables: JUL_AUG JUL_SEP JUL_OCT AUG_SEP AUG_OCT NAY_JUN MAY_JUL HAY_AUG JUN_AUG

Pearson Correlation Coefficients / Prob > |R| under Ho: Rho»0 / Number of Observations

	JUL_AUG	JUL_SEP	JUL_OCI	AU0_SEP	AU0_OCT	MAY_JUM	HAY_JUL	MAYJAUG	JUN_AUG
LOU	0.07736	0.20610	0.23351	0.37392	0.36357	0.11781	0.11696	0.18906	0.23823
	0.4843	0.0600	0.0325	0.0005	0.0007	0.2858	0.2894	0.0850	0.0291
	84	84	84	84	84	84	84	84	84
MID	-0.03354	0.10893	0.20968	0.27319	0.34010	0.28920	0.20637	0.21669	0121478
	0.7496	0.2986	0.0437	0.0081	0.0009	0.0047	0.0460	0.0359	0.0376
	93	93	93	93	93	94	94	94	94
HI	0.10091	0.21066	0.29387	0.42598	0.45970	0.38141	0.29884	0.39186	0136039
	0.3358	0.0427	0.0042	0.0001	0.0001	0.0001	0.0034	0.0001	0.0004
	93	93	93	93	93	94	94	94	94

Table C.l Correlation coefficients, and their level of significance, for standardized ring width and Illinois regional precipitation (climate division 8).
Low = floodplain; mid = mid-slope; hi = high-level;
prefix L = last year.

Anna precipitation

Pearson Correlation Coefficients / Prob > |R| under Ho: Rho = 0 / Number of Observations

	LMAYP	LJUNP	LJULP	LAUGP	LSEPP	LOCTP	LNOVP	LDECP	JAHP	FEBP
LOU	0.07279	0.00682	-0.27357	0.26364	0.23476	0.04165	-0.17285	0.05272	0.10447	-0.21057
	0.5028	0.9503	0.0104	0.0136	0.0286	0.7017	0.1094	0.6277	0.3356	0.0503
	87	86	87	87	87	87	87	87	87	87
HID	0.11250	0.18699'	-0.20658	0.10613	0.17544	0.08332	0.07651	0.09675	0.14595	-0.00482
	0.2911	0.0793	0.0508	0.3195	0.0981	0.4350	0.4735	0.3643	0.1675	0.9638
	90	89	90	90	90	90	90	90	91	91
HI	0.08351	0.07884	-0.27474	0.31760	0.21222	0.09300	-0.01573	0.22800	0.16041	-0.00778
	0.4339	0.4627	0.0088	0.0023	0.0446	0.3833	0.8830	0.0307	0.1288	0.9417
	90	89	90	90	90	90	90	90	91	91

	HARP	APRP	HAYP	JUNP	JULP	AUGP	SEPP	OCTP	NOVP	DECP
LOU	0.24676	-0.06349	0.07944	0.16065	0.104458	0.09790	-0.03523	-0.05624	0.00923	-0.01174
	0.0220	0.5591	0.4645	0.1395	0.6818	0.3670	0.7460	0.6049	0.9324	0.9140
	86	87	87	86	87	87	87	87	87	87
HID	0.08879	0.05840	0.23315	0.42178	-0.03877	-0.00995	-0.04792	0.14444	0.01455	-0.05756
	0.4053	0.5824	0.0261	0.0001	0.7152	0.9254	0.6519	0.1719	0.8911	0.5878
	90	91	91	90	91	91	91	91	91	91
HI	0.02539	0.04086	0.28071	0.34806	0.04206	0.09656	-0.05664	0.15194	-0.12724	-0.02361
	0.8123	0.7006	0.0070	0.0008	0.6922	0.3626	0.5938	0.1505	0.2294	0.8242
	90	91	91	90	91	91	91	91	91	91

3 'WITH' Variables: LOU HID HI
9 'VAR' Variables: JUL_AUG JUL_SEP JUL_OCI AUG_SEP AUG_OCT HAY_JUN HAY_JUL HAY_AUG JUN_AUG

Pearson Correlation Coefficients / Prob > |R| under Ho: Rho= 0 / Number of Observations

	JUL_AUG	JUL_SEP	JUL_OCT	AUGSEP	AUG_OCT	HAY_JUN	HAY_JUL	HAY_AUG	JUNAUG
LOU	-0.00570	0.13800	0.14724	0.35881	0.33570	0.17951	0.17477	0.22604	0.21107
	0.9582	0.2024	0.1735	0.0006	0.0015	0.0982	0.1075	0.0364	0.0511
	87	87	87	87	87	86	86	86	86
HID	-0.07863	0.04292	0.08496	0.20109	0.22563	0.44973	0.35582	0.33649	0.25912
	0.4613	0.6879	0.4259	0.0574	0.0325	0.0001	0.0006	0.0012	0.0137
	90	90	90	90	90	90	90	90	90
HI	0.03537	0.15754	0.19263	0.38307	0.38880	0.43732	0.38713	0.42440	0.32975
	0.7406	0.1381	0.0689	0.0002	0.0002	0.0001	0.0002	0.0001	0.0015
	90	90	90	90	90	90	90	90	90

Table C.2 Correlation coefficients, and their level of significance, for standardized ring width and Anna precipitation.
Low = floodplain; mid = mid-slope; hi = high-level;
prefix L = last year.

Carbondale precipitation

Pearson Correlation Coefflcients / Prob > |R| under Ho: Rho=0 / Number of Observations

	LHAYP	LJUNP	LJULP	LAUGP	LSEPP	LOCTP	LNOVP	LDECP	JANP	FEBP
LOU	-0.07432	-0.07723	-0.15413	0.31587	0.22902	-0.00487	0.05936	0.10057	0.13335	-0.11204
	0.5179	0.4959	0.1722	0.0043	0.0410	0.9665	0.6009	0.3810	0.2414	0.3256
	78	80	80	80	80	77	80	78	79	79
HID	0.01306	-0.02278	-0.23789	0.16818	0.25081	0.05022	0.15606	0.07531	0.09456	0.07021
	0.9097	0.8410	0.0336	0.1359	0.0248	0.6645	0.1669	0.5123	0.4071	0.5386
	78	80	80	80	80	77	80	78	79	79
HI	0.08001	-0.09495	-0.27189	0.44815	0.24212	0.11329	0.15233	0.22409	0.16363	0.01782
	0.4862	0.4021	0.0147	0.0001	0.0305	0.3266	0.1774	0.0486	0.1496	0.8761
	78	80	80	80	80	77	80	78	79	79

	HARP	APRP	HAYP	JUMP	JULP	AUGP	SEPP	OCTP	NOVP	DECP
LOU	0.35645	0.04005	-0.01648	0.24497	0.04549	0.21871	-0.08401	-0.19418	-0.06751	0.04294
	0.0011	0.7226	0.8861	0.0275	0.6867	0.0498	0.4559	0.0885	0.5493	0.7071
	81	81	78	81	81	81	81	78	81	79
HID	0.13057	0.09849	0.09218	0.39256	-0.07824	0.02240	-0.01184	0.02577	-0.03630	-0.03308
	0.2453	0.3817	0.4221	0.0003	0.4875	0.8427	0.9164	0.8228	0.7476	0.7723
	81	81	78	81	81	81	81	78	81	79
HI	0.09286	0.04005	0.18731	0.44922	0.07792	0.27640	0.03345	0.06435	-0.13912	0.05201
	0.4096	0.7226	0.1006	0.0001	0.4893	0.0125	0.7668	0.5757	0.2155	0.6489
	81	81	78	81	81	81	81	78	81	79

3 'WITH' Varlables: LOU HID HI
9 'VAR' Varlables: JUL_AUG JUL_SEP JUL_OCT AUG_SEP AUG_OCT HAY_JUM HAY_JUL HAY_ AUG JUN_AUG

Pearson Correlation Coefficients / Prob » |R| under Ho: Rho=0 / Number of Observatlons

	JUL_AUG	JUL_SEP	JUL _OCT	AUG_SEP	AUG_OCT	HAV_JUN	HAY_JUL	HAY_AUG	JUN_AUG
LOU	0.14856	0.24961	0.20635	0.36669	0.30063	0.14295	0.12949	0.20103	0.29542
	0.1885	0.0265	0.0718	01.0009	0.0079	0.2118	0.2585	0.0776	0.0074
	80	79	77	79	77	78	78	78	81
HID	-0.02526	0.11947	0.13702	0.27756	0.27429	0.35216	0.24408	0.23063	0.22203
	0.8240	0.2943	0.2347	t1.0133	0.0158	0.0016	0.0313	0.0422	0.0464
	80	79	77	79	77	78	78	78	81
HI	0.17513	0.28320	0.30745	0.47910	0.47428	0.46837	0.40932	0.50583	0.47027
	0.1202	0.0114	0.0065	0.0001	0.0001	0.0001	0.0002	0.0001	0.0001
	80	79	77	79	77	78	78	78	81

Table C.3 Correlation coefficients, and their level of significance, for standardized ring width and Carbondale precipitation.
Low = floodplain; mid = mid-slope; hi = high-level;
prefix L = last year.

Illinois regional temperature

Pearson Correllat i on Coe fficients / Prob > |R| under Ho: Rho= 0 / Number of Observati ons

	LHAYT	LJUNT	LJULT	LAUGT	LSEPT	LOCTT	LNOVT	LDECT	JANT	FEBT
LOW	0.11904	0.02088	0.04432	-0.18147	-0.07166	0.10339	-0.18610	-0.02190	-0.09451	-0.04691
	0.2808	0.8505	0.6889	0.0985	0.5171	0.3493	0.0901	0.8433	0.3925	0.6718
	84	84	84	84	84	84	84	84	84	84
MIP	-0.00298	0.06625	0.10055	0.01352	0.02967	0.17743	0.00270	0.16298	0.09551	0.32122
	0.9774	0.5281	0.3376	0.8977	0.7777	0.0889	0.9795	0.1185	0.3598	0.0016
	93	93	93	93	93	93	93	93	94	94
HI	-0.06510	0.01764	0.06427	-0.09547	-0.12084	0.12406	0.14035	0.07546	0.06275	0.24923
	0.5353	0.8667	0.5405	0.3627	0.2486	0.2361	0.1796	0.4722	0.5480	0.0154
	93	93	93	93	93	93	93	93	94	94

	HART	APRI	HAYT	JUNT	JULT	AUGT	SEPT	OCTT	NOVT	DECT
LOU	-0.02253	0.10242	0.04347	-0.22841	-0.13917	0.11995	0.14257	0.12404	0.16518	0.13206
	0.8388	0.3539	0.6946	0.0366	0.2068	0.2771	0.1958	0.2610	0.1332	0.2311
	84	84	84	84	84	84	84	84	84	84
HID	0.10499	0.08969	-0.15828	-0.16659	-0.01488	0.05364	0.04852	0.09613	0.03949	0.09123
	0.3139	0.3900	0.1276	0.10B5	0.8868	0.6076	0.6424	0.3567	0.7055	0.3819
	94	94	94	94	94	94	94	94	94	94
HI	0.11814	0.07826	-0.31816	-0.37097	-0.08562	0.10501	0.10222	0.14288	0.12205	0.12511
	0.2568	0.4534	0.0018	0.0002	0.4119	0.313B	0.3269	0.1695	0.2413	0.2296
	94	94	94	94	94	94	94	94	94	94

3 'WITH' Variables: LOU HID HI
3 'VAR' Variables: HAT _JUN HAT_JUL JUN_JUL

Pearson Correlation Coefficients / Prob > |R| 'under Ho: Rho:=0 / Number of Observati ons

	HAY_JUN	HAY_JUL	JUN_JUL
LOU	-0.10681	-0.14194	-0.23407
	0.3335	0.1978	0.0321
	84	84	84
HID	-0.21232	-0.17748	-0.12134
	0.0399	0.0870	0.2440
	94	94	94
HI	-0.44884	-0.39736	-0.29974
	0.0001	0.0001	0.0033
	94	94	94

Table C.4 Correlation coefficients, and their level of significance, for standardized ring width and Illinois regional temperature (climate division 8).
Low = floodplain; mid = mid-slope; hi = high-level;
prefix L = last year.

Anna temperature

Pearson Correlation Coefficients / Prob > |R| under Ho: Rho=0 / Number of Observations

	LMAYT	LJUNI	LJULT	LAUGT	LSEPT	LOCTT	LNOVT	LDECY	JANT	FEBT
LOU	0.11073 0.3072 87	-0.01071 0.9220 86	-0.00912 0.9332 87	-0.17835 0.1004 86	-0.06822 0.5301 87	0.11355 0.2950 87	-0.20989 0.0510 87	0.04416 0.6847 87	-0.13751 0.2041 87	-0.08739 0.4209 87
HID	-0.01429 0.8937 90	0.00300 0.9777 89	-0.03726 0.7274 90	-0.07019 0.5133 89	-0.09468 0.3747 90	0.09097 0.3938 90	-0.23431 0.0262 90	0.12453 0.2422 90	0.04815 0.6504 91	0.22430 0.0326 91
HI	-0.09184 0.3893 90	0.04093 0.7034 89	0.03286 0.7585 90	-0.15463 0.1479 89	-0.15876 0.1350 90	0.06497 0.5429 90	0.04476 0.6753 90	0.08391 0.4317 90	0.04063 0.7022 91	0.15713 0.1369 91
	HART	APRT	MAYT	JUNT	JULT	AUGT	SEPT	OCTT	NOVT	DECT
LOW	-0.07073 0.5175 86	0.03241 0.7657 87	-0.02107 0.8464 87	-0.23254 0.0312 86	-0.15483 0.1522 87	-0.14064 0.1965 86	0.00129 0.9905 87	-0.07969 0.4631 87	0.07165 0.5096 87	-0.00450 0.9670 87
MID	-0.03585 0.7372 90	0.02740 0.7966 91	-0.20815 0.0477 91	-0.28774 0.0060 90	-0.20884 0.0470 91	-0.12137 0.2545 90	-0.16575 0.1164 91	0.12366 0.2429 91	-0.30384 0.0034 91	0.06969 0.5116 91
HI	0.01792 0.8669 90	0.08075 0.4467 91	-0.37630 0.0002 91	-0.44544 0.0001 90	-0.17672 0.0938 91	-0.20049 0.0581 90	-0.12597 0.2341 91	0.14381 0.1739 91	-0.10003 0.3455 91	0.01782 0.8669 91

3 'WITH ' Variables: LOU MID HI
3 'VAR' Variables: MAY_JUN HAY_JUL JUN_JUL

Pearson Correlation Coefficients / Prob > |Ft| under Ho: Rho = 0 / Number of Observations

	MAY_JUN	HAY_JUL	JUN_JUL
LOU	-0.15164 0.1634 86	-0.17814 0.1008 86	-0.23853 0.0270 86
MID	-0.30595 0.0034 90	-0.32088 0.0020 90	-0.30432 0.0035 90
HI	-0.51317 0.0001 90	-0.47064 0.0001 90	-0.38955 0.0001 90

Table C.5 Correlation coefficients, and their level of significance, for standardized ring width and Anna temperature.

Low = floodplain; mid = mid-slope; hi = high-level;
prefix L = last year.

Carbondale temperature

Pearson Correlation Coefficients / Prob > |R| under Ho: Rho = 0 / Number of Observations

	LMATT	LJUNT	LJULT	LAUGT	LSEPT	LOCTT	LNOVT	LDECT	JANT	FEBT
LOU	0.21408	0.06269	-0.00283	-0.10064	0.04345	0.14741	-0.08653	0.02194	-0.03409	0.04779
	0.0598	0.5806	0.9801	0.3744	0.7019	0.1978	0.4454	0.8488	0.7655	0.6758
	78	80	80	80	80	78	80	78	79	79
MID	0.03707	0.06810	0.06259	0.07888	0.09084	0.19661	0.06006	0.17138	0.19127	0.25418
	0.74 73	0.5484	0.5812	0.4867	0.4229	0.0845	0.5967	0.1335	0.0913	0.0238
	78	80	80	80	80	78	80	78	79	79
HI	-0.02360	0.04863	0.06150	-0.05871	-0.03059	0.12279	0.17458	0.09031	0.12579	0.13231
	0.8375	0.6684	0.5879	0.6050	0.7876	0.2842	0.1214	0.4317	0.2693	0.2451
	78	80	80	80	80	78	80	78	79	79

	HART	APRT	MAYT	JUHT	JULT	AUGT	SEPT	OCTT	NOVT	DECT
LOU	-0.06173	0.05024	0.03312	-0.27929	-0.15961	-0.17581	-0.05392	-0.08162	0.20824	0.01018
	0.5865	0.6560	0.7720	0.0116	0.1547	0.1164	0.6326	0.4746	0.0621	0.9291
	80	81	79	81	81	81	81	79	81	79
HID	0.10529	0.03354	-0.14834	-0.23419	-0.14433	-0.00234	-0.05888	0.21231	-0.06328	0.07289
	0.3526	0.7662	0.1920	0.0354	0.1986	0.9835	0.6015	0.0603	0.5746	0.5232
	80	81	79	81	81	81	81	79	81	79
HI	0.05906	0.05467	-0.27390	-0.42062	-0.18772	-0.19472	-0.12843	0.10865	-0.01683	-0.01797
	0.6028	0.6278	0.0146	0.0001	0.0933	0.0815	0.2532	0.3405	0.8814	0.8751
	80	81	79	81	81	81	81	79	81	79

3 'WITH' Variables: LOU MID HI
3 'VAR' Variables: MAY_JUN MAY_JUL JUN_JUL

Pearson Correlation Coefficients / Prob > |R| under Ho: Rho=0 / Number of Observations

	HAY_JUM	HAY_JUL	JUN_JUL
LOU	0.12550	-0.15159	-0.27386
	0.2704	0.1823	0.0134
	79	79	81
HID	-0.23680	-0.24477	-0.23553
	0.0356	0.0297	0.0343
	79	79	81
HI	-0.42996	-0.40742	-0.38289
	0.0001	0.0002	0.0004
	79	79	81

Table C.6 Correlation coefficients, and their level of significance, for standardized ring width and Carbondale temperature.
Low = floodplain; mid = mid-slope; hi = high-level;
prefix L = last year.

Illinois regiona1 PDSI

Pearson Correlation Coefficlents / Prob > |R| under Ho: Rho=0 / Number of Observations

	LMAYS	LJUNS	LJULS	LAUGS	LSEPS	LOCTS	LNOVS	LDECS	JANS	FEBS
LOU	0.00759 0.9460 82	-0.00533 0.9621 82	-0.04768 0.6706 82	0.11783 0.2918 82	0.20913 0.0594 82	0.20764 0.0612 82	0.22416 0.0429 82	0.24828 0.0245 82	0.24408 0.0271 82	0.21065 0.0575 82
HID	0.08222 0.4385 91	0.10078 0.3418 91	0.00231 0.9827 91	0.07472 0.4815 91	0.26813 0.0102 91	0.32032 0.0020 91	0.32996 0.0014 91	0.30920 0.0029 91	0.28509 0.0059 92	0.26635 0.0103 92
HI	0.13255 0.2104 91	0.14884 0.1591 91	0.04385 0.6798 91	0.18859 0.0734 91	0.32455 0.0017 91	0.37432 0.0003 91	0.39876 0.0001 91	0.40897 0.0001 91	0.37354 0.0002 92	0.33344 0.0012 92

	MARS	APRS	MAYS	JUNS	JULS	AUGS	SEPS	OCTS	NOVS	DECS
LOU	0.31523 0.0039 82	0.24244 0.0282 82	0.19696 0.0761 82	0.23333 0.0349 82	0.24708 0.0252 82	0.24043 0.0306 81	0.12521 0.2654 81	0.08340 0.4592 81	0.11914 0.2894 81	0.08828 0.4332 81
MID	0.24633 0.0179 92	0.30593 0.0030 92	0.27994 0.0069 92	0.32037 0.0018 92	0.23131 0.0265 92	0.21382 0.0418 91	0.21684 0.0390 91	0.23821 0.0230 91	0.21719 0.0386 91	0.16447 0.1193 91
HI	0.30812 0.0028 92	0.37105 0.0003 92	0.45604 0.0001 92	0.46659 0.0001 92	0.38251 0.0002 92	0.40889 0.0001 91	0.35414 0.0006 91	0.35555 0.0005 91	0.29938 0.0039 91	0.24220 0.0207 91

Table C.7 Correlation coefficients, and their level of significance, for standardized ring width and Illinois regional PDSI (climate division 8).
Low = floodplain; mid = mid-slope; hi = high-level;
prefix L = last year.

Illinois regional PHDI

Pearson Correlation Coefficients / Prob > |R| under Ho: Rho=0 / Number of Observations

	LMAYH	LJUNH	LJULH	LAUGH	LSEPH	LOCTH	LNOVH	LOECH	JANH	FEBH
LOU	-0.00081	-0.01457	-0.07381	0.02573	0.10712	0.17259	0.18108	0.18058	0.20085	0.16444
	0.9942	0.8960	0.5073	0.8174	0.3351	0.1187	0.1014	0.1023	0.0686	0.1374
	83	83	83	83	83	83	83	83	83	83
HID	0.00928	0.05199	-0.02993	-0.00782	0.08999	0.15719	0.23297	0.24080	0.21402	0.20654
	0.9300	0.6226	0.7770	0.9410	0.3936	0.1345	0.0254	0.0208	0.0394	0.0470
	92	92	92	92	92	92	92	92	93	93
HI	0.03146	0.04464	-0.04949	0.06569	0.15725	0.21686	0.29236	0.31828	0.30545	0.29807
	0.7659	0.6727	0.6395	0.5339	0.1344	0.03 79	0.0047	0.0020	0.0029	0.0037
	92	92	92	92	92	92	92	92	93	93
	HARH	APRH	MAYH	JUNH	JULH	AUGH	SEPH	OCTH	NOVH	DECH
LOU	0.29444	0.28651	0.22479	0.23013	0.24296	0.22834	0.22127	0.18603	0.19731	0.18585
	0.0069	0.0086	0.0410	0.0364	0.0269	0.0391	0.0457	0.0943	0.0756	0.0946
	83	83	83	83	83	82	82	82	82	82
HID	0.19261	0.23070	0.25814	0.33859	0.28931	0.24475	0.25741	0.29865	0.30121	0.26441
	0.0644	0.0261	0.0125	0.0009	0.0049	0.0187	0.0132	0.0038	0.0035	0.0109
	93	93	93	93	93	92	92	92	92	92
HI	0.27905	0.30397	0.38370	0.44941	0.40729	0.43412	0.46066	0.49062	0.45650	0.39342
	0.0068	0.0031	0.0001	0.0001	0.0001	0.0001	0.0001	0.0001	0.0001	0.0001
	93	93	93	93	93	92	92	92	92	92

Table C.8 Correlation coefficients, and their level of significance, for standardized ring width and Illinois regional PHDI (cliamte division 8).
Low = floodplain; mid = mid-slope; hi = high-levels-
prefix L = last year.

Murphysboro discharge

3 'WITH' Variables: LOU MID HI
12 'VAR' Variables: LOCT LNOV LDEC JAN FEB MAR APR MAY JUKI Jul AUG SEP

Pearson Correlation Coefficients / Prob > |R | under Ho: Rho=0 / Number of Observations

	LOCT	LNOV	LDEC	JAN	FEB	HAR	APR	HAY	JUN	JUL	AUG	SEP
LOU	0.16717	0.46196	0.43498	0.12305	0.16301	0.33627	0.23748	0.04594	0.11407	0.13686	0.07062	0.00201
	0.1978	0.0002	0.0005	0.3448	0.2094	0.0081	0.0653	0.7252	0.3814	0.2929	0.5886	0.9877
	61	61	61	61	61	61	61	61	61	61	61	61
MID	0.13S74	0.27534	0.07703	0.37859	0.32414	0.15514	0.15229	0.04905	0.16543	0.06282	0.17713	0.14667
	0.2969	0.0317	0.5552	0.0026	0.0108	0.2325	0.2413	0.7074	0.2026	0.6305	0.1721	0.2593
	61	61	61	61	61	61	61	61	61	61	61	61
HI	0.17441	0.38872	0.29559	0.37352	0.28924	0.24201	0.22706	0.09457	0.23423	0.15016	0.16986	0.27755
	0.1788	0.0020	0.0207	0.0030	0.0238	0.0602	0.07B4	0.4685	0.0692	0.2481	0.1906	0.0303
	61	61	61	61	61	61	61	61	61	61	61	61

Pearson Correlat1on Coefficients / Prob > |R| under Ho: Rho=0 / Number of Observations

	NDV_DEC	NOV_JAN	NOV_FEB	H0V_HAR	NOV _APR	DEC_JAN	DEC_FEB	DEC_MAR
LOU	0.51877	0.36765	0.33254	0.40722	0.42086	0.28369	0.26691	0.35820
	0.0001	0.0036	0.0088	0.0011	0.0007	0.0267	0.03 76	0.0046
	61	61	61	61	61	61	61	61
MID	0.18201	0.35170	0.38214	0.38583	0.37577	0.32009	0.35924	0.36804
	0.1604	0.0054	0.0024	0.0021	0.0028	0.0119	0.0045	0.0035
	61	61	61	61	61	61	61	61
HI	0.38737	0.46153	0.44967	0.47512	0.47522	0.41204	0.40941	0.44445
	0.0020	0.0002	0.0003	0.0001	0.0001	0.0010	0.0011	0.0003
	61	61	61	61	61	61	61	61

	DEC_APR	JAN_FEB	JAN_MAR	JAN_APR	FEB _MAR	FEB_APR	HAR_APR
LOU	0.37769	0.15342	0.27431	0.30992	0.32715	0.33929	0.32592
	0.0027	0.2378	0.0324	0.0151	0.0101	0.0075	0.0104
	61	61	61	61	61	61	61
MID	0.35739	0.38722	0.39226	0.37429	0.30592	0.28358	0.17530
	0.0047	C1.0020	0.0018	0.0030	0.0165	0.0268	0.1766
	61	61	61	61	61	61	61
HI	0.44602	0.36743	0.41322	0.41880	0.34249	0.34479	0.26734
	0.0003	t1.0036	0.0009	0.0008	0.0069	0.0065	0.0373
	61	61	61	61	61	61	61

Table C.9 Correlation coefficients, and their level of significance, for standardized ring width and Murphysboro discharge.

Low = floodplain; mid = mid-slope; hi = high-level;
prefix L = last year.

Thebes discharge

3 'WITH' Variables: LOU HID HI
12 'VAR' Variables: LOCT LNOV LDEC JAN FEB MAR APR MAY JUN JUL AUG SEP

Pearson Correlation Coefficients / Prob > |R| Under Ho: Rho=0 / Number of Observations

	LOCT	LNOV	LDEC	JAN	FEB	MAR	APR	MAY	JUN	JUL	AUG	SEP
LOU	0.32152	0.28927	0.17069	0.34568	0.36556	0.49695	0.42818	0.35482	0.22420	0.26765	0.21413	0.19073
	0.0157	0.0306	0.2085	0.0091	0.0056	0.0001	0.0009	0.0068	0.0936	0.0441	0.1097	0.1553
	56	56	56	56	56	56	57	57	57	57	57	57
MID	0.29013	0.32923	-0.00917	0.29513	0.23660	0.23839	0.10755	0.12766	0.36437	0.36833	0.02381	-0.13470
	0.0301	0.0132	0.9465	0.0272	0.0792	0.0768	0.4259	0.3440	0.0053	0.0048	0.8604	0.3178
	56	56	56	56	56	56	57	57	57	57	57	57
HI	0.32187	0.17589	0.04017	0.45522	0.39242	0.45276	0.34618	0.37052	0.50442	0.47015	0.23955	0.06898
	0.0156	0.1947	0.7688	0.0004	0.0028	0.0005	0.0083	0.0046	0.0001	0.0002	0.0727	0 .6102
	56	56	56	56	56	56	57	57	57	57	57	57

Table C.10 Correlation coefficients, and their level of significance, for standardized ring width and Anna precipitation.
Low = floodplain; mid = mid-slope; hi = high-level;
prefix L = last year.

(continued on pages 99 and 100)

Correlation Analysis

Pearson Correlation Coefficients / Prob > |R| under Ho:: Rho=0 / Number of Observations

	OCT_NOV	OCT_DEC	OCT_JAN	OCT_FEB	OCTHAR	OCT_APR	OCT_HAY	OCT_JUH	OCT_JUL	OCT_AUG	OCT_SEP
LOU	0.38850	0.38508	0.41607	0.43623	0.49354	0.53094	0.53400	0.51683	0.51822	0.51736	0.52060
	0.0031	0.0034	0.0014	0.0008	0.0001	0.0001	0.0001	0.0001	0.0001	0.0001	0.0001
	56	56	56	56	56	56	56	56	56	56	56
HID	0.39569	0.30350	0.33310	0.33719	0.34459	0.31960	0.30200	0.33646	0.37008.	0.36176	0.34478
	0.0025	0.0230	0.0121	0.0110	0.0093	0.0163	0.0237	0.0112	0.0050	0.0062	0.0093
	56	56	56	56	56	56	56	56	56	56	56
HI	0.31372	0.26362	0.33462	0.37199	0.42820	0.45542	0.47093	0.51376	0.55113	0.55311	0.54839
	0.0185	0.0496	0.0117	0.0048	0.0010	0.0004	0.0002	0.0001	0.0001	0.0001	0.0001
	56	56	56	56	56	56	56	56	56	56	56

	NOV_DEC	NOV_JAM	NOV_FEB	NOV_HAR	NOV_APR	NOV_HAY	NOV_JUN	NOV_JUL	NOV_AUG	MOV_SEP	DEC_JAN
LOU	0.30434	0.35747	0.39022	0.46120	0.50217	0.50726	0.49381	0.49631	0.49554	0.49863	0.28499
	0.0226	0.0068	0.0029	0.0003	0.0001	0.0001	0.0001	0.0001	0.0001	0.0001	0.0333
	56	56	56	56	56	56	56	56	56	56	56
HID	0.21685	0.26882	0.28343	0.29885	0.27472	0.26084	0.30425	0.34267	0.33420	0.31604	0.11936
	0.1084	0.0451	0.0343	0.0253	0.0405	0.0522	0.0226	0.0097	0.0118	0.0176	0.3809
	56	56	56	56	56	56	56	56	56	56	56
HI	0.14455	0.25391	0.31190	0.38500	0.41759	0.43813	0.49039	0.53173	0.53390	0.52834	0.22756
	0.2878	0.0590	0.0193	0.0034	0.0014	0.0007	0.0001	0.0001	0.0001	0.0001	0.0917
	56	56	56	56	56	56	56	56	56	56	56

	DEC_FEB	DEC_HAR	0EC_APR	DEC_HAY	DEC_JUN	DEC_JUL	DEC_AUG	DEC_SEP	JAN_FEB	JAN_HAR	JAN_APR
LOU	0.35227	0.44672	0.48833	0.49091	0.47486	0.47641	0.47504	0.47741	0.37953	0.47701	0.50412
	0.0078	0.0006	0.0001	0.0001	0.0002	0.0002	0.0002	0.0002	0.0039	0.0002	0.0001
	56	56	56	56	56	56	56	56	56	56	56
HID	0.17785	0.22085	0.20494	0.19927	0.25400	0.29921	0.29074	0.27129	0.28191	0.29093	0.24402
	0.1897	0.1019	0.1297	0.1409	0.0589	0.0251	0.0297	0.0431	0.0353	0.0296	0.0699
	56	56	56	56	56	56	56	56	56	56	56
HI	0.31779	0.40466	0.42960	0.44580	0.50003	0.54117	0.54181	0.53388	0.45016	0.49952	0.48768
	0.0170	0.0020	0.0010	0.0006	0.0001	0.0001	0.0001	0.0001	0.0005	0.0001	0.0001
	56	56	56	56	56	56	56	56	56	56	56

Table C.10 (continued)

Correlation Analysis

Pearson Correlation Coefficients / Prob > |R| under Ho:: Rho=0 / Number of Observations

	JAN_HAY	JAH_JUN	JAN_JUL	JAN_AUG	JAH_SEP	FEB_HAR	FEB_APR	FEB_MAY	FEB_JUN	FEB_JUL	FEB_AUG
LOU	0.49630 0.0001 56	0.47138 0.0002 56	0.46834 0.0003 56	0.46528 0.0003 56	0.46633 0.0003 56	0.48997 0.0001 56	0.50933 0.0001 56	0.49586 0.0001 56	0.46561 0.0003 56	0.45986 0.0004 56	0.45624 0.0004 56
HID	0.22580 0.0943 56	0.27839 0.0377 56	0.32093 0.0159 56	0.30979 0.0202 56	0.28757 0.0316 56	0.26335 0.0499 56	0.21390 0.1134 56	0.19966 0.1401 56	0.26095 0.0521 56	0.30734 0.0212 56	0.29552 0.0270 56
HI	0.48632 0.0001 56	0.53284 0.0001 56	0.56739 0.0001 56.	0.56470 0.0001 56	0.55354 0.0001 56	0.47385 0.0002 56	0.46185 0.0003 56	0.46398 0.0003 56	0.51637 0.0001 56	0.55225 0.0001 56	0.54920 0.0001 56
	FEB_SEP	HAR_APR	MAR_HAY	HAR_JUN	HAR_JUL	HAR_AUG	HAR_SEP	APR_HAY	APR_JUN	APR_JUL	APR_AUG
LOU	0.45645 0.0004 56	0.50268 0.0001 56	0.48392 0.0002 56	0.45142 0.0005 56	0.44565 0.0006 56	0.44184 0.0007 56	0.44182 0.0007 56	0.41860 0.0012 57	0.38719 0.0029 57	0.38721 0.0029 57	0.38693 0.0029 57
HID	0.27148 0.0430 56	0.18231 0.1787 56	0.17360 0.2007 56	0.24698 0.0665 56	0.29909 0.0251 56	0.28622 0.0325 56	0.26000 0.0530 56	0.12486 0.3548 57	0.22194 0.0971 57	0.28146 0.0339 57	0.26637 0.0452 57
HI	0.53634 0.0001 56	0.43470 0.0008 56	0.44083 0.0007 56	0.50308 0.0001 56	0.54267 0.0001 56	0.53909 0.0001 56	0.52453 0.0001 56	0.38124 0.0034 57	0.46006 0.0003 57	0.50221 0.0001 57	0.49753 0.0001 57
	APR_SEP	HAY_JUN	MAY_JUL	HAY_AUG	HAY_SEP	JUN_JUL	JUN_AUG	JUN_SEP	JUL_AUG	JUL_SEP	AUG_SEP
LOU	0.38920 0.0028 57	0.31659 0.0164 57	0.32776 0.0128 57	0.32963 0.0123 57	0.33566 0.0107 57	0.26978 0.0424 57	0.27858 0.0359 57	0.29059 0.0283 57	0.27160 0.0410 57	0.28057 0.0345 57	0.23124 0.0835 57
HID	0.23566 0.0776 57	0.26455 0.0467 57	0.32711 0.0130 57	0.30130 0.0228 57	0.25924 0.0515 57	0.40262 0.0019 57	0.35551 0.0066 57	0.29205 0.0275 57	0.28505 0.0316 57	0.19238 0.1517 57	-0.06937 0.6081 57
HI	0.47907 0.0002 57	0.47413 0.0002 57	0.51636 0.0001 57	0.50505 0.0001 57	0.47992 0.0002 57	0.53601 0.0001 57	0.51563 0.0001 57	0.47867 0.0002 57	0.43235 0.0008 57	0.37511 0.0040 57	0.17063 0.2044 57

Table C.10 (continued)

Appendix D

Standardized indices for chronologies

Listed are ring growth years, and corresponding standardized dimensionless indices for the floodplain (LOW), mid-slope (MID), and high-level (HIGH) chronologies.

Year	LOW	MID	HIGH	Year	LOW	MID	HIGH	Year	LOW	MID	HIGH
1870			205	1911	57	46	71	1952	131	103	95
1871			150	1912	154	73	121	1953	79	94	87
1872			65	1913	146	39	79	1954	93	104	92
1873			60	1914	97	42	75	1955	109	136	122
1874			46	1915	140	71	132	1956	82	108	99
1875			76	1916	104	70	123	1957	103	111	99
1876			59	1917	110	91	115	1958	103	113	105
1877			90	1918	82	60	84	1959	82	101	87
1878			94	1919	72	102	109	1960	110	108	106
1879			145	1920	124	92	113	1961	97	92	86
1880			121	1921	121	85	102	1962	97	95	82
1881			113	1922	124	172	124	1963	83	84	69
1882			72	1923	91	146	121	1964	86	85	74
1883			93	1924	97	157	146.	1965	111	103	93
1884			117	1925	95	118	115	1966	88	101	92
1885			59	1926	91	109	90	1967	104	105	102
1886			44	1927	112	175	122	1968	119	123	109
1887			43	1928	106	200	141	1969	98	110	108
1888			46	1929	90	150	133	1970	98	102	98
1889			55	1930	84	108	108	1971	97	97	95
1890			49	1931	88	119	123	1972	98	93	90
1891			46	1932	98	135	126	1973	117	120	125
1892		85	108	1933	93	119	119	1974	108	121	133
1893		63	75	1934	77	103	88	1975	133	114	132
1894		49	78	1935	122	171	139	1976	119	97	118
1895		46	62	1936	91	115	92	1977	112	90	102
1896		48	70	1937	105	167	107	1978	107	86	114
1897		43	64	1938	117	174	129	1979	87	93	104
1898		45	83	1939	95	140	99	1980	81	83	90
1899		66	76	1940	86	109	93	1981	72	66	78
1900		52	75	1941	73	86	74	1982	104	87	99
1901		40	72	1942	90	127	106	1983	114	103	98
1902		40	76	1943	79	112	106	1984	100	107	112
1903		69	106	1944	100	101	91	1985	133	124	128
1904		66	88	1945	116	134	123	1986	121	116	118
1905	153	62	92	1946	103	150	122	1987	107	95	94
1906	114	57	80	1947	97	150	134	1988	75	81	78
1907	95	85	107	1948	107	129	112	1989	74	102	106
1908	92	53	92	1949	95	141	118	1990	74	96	107
1909	57	50	106	1950	95	122	115	1991	83	103	120
1910	64	60	112	1951	118	161	138				